

## Article

# Influence of Red Mud Catalyst and Reaction Atmosphere on Hydrothermal Liquefaction of Algae

Tawsif Rahman <sup>1</sup>, Hossein Jahromi <sup>1,2</sup>, Poulami Roy <sup>1</sup>, Sushil Adhikari <sup>1,2,\*</sup>, Farshad Feyzbar-Khalkhali-Nejad <sup>3</sup>, Tae-Sik Oh <sup>3</sup>, Qichen Wang <sup>1</sup> and Brendan T. Higgins <sup>1</sup>

<sup>1</sup> Biosystems Engineering Department, 200 Corley Building, Auburn University, Auburn, AL 36849, USA

<sup>2</sup> Center for Bioenergy and Bioproducts, 519 Devall Drive, Auburn University, Auburn, AL 36849, USA

<sup>3</sup> Department of Chemical Engineering, 346 Ross Hall, Auburn University, Auburn, AL 36849, USA

\* Correspondence: sza0016@auburn.edu

**Abstract:** Algae are a diverse group of aquatic organisms and have a potential to produce renewable biofuel via hydrothermal liquefaction (HTL). This study investigated the effects of reaction environments on biocrude production from “*Tetraselmis* sp.” algae strain by HTL process using red mud (RM) based catalyst. The inert (N<sub>2</sub>), ethylene (C<sub>2</sub>H<sub>4</sub>), reducing (10% H<sub>2</sub>/90% N<sub>2</sub>), and oxidizing (10% O<sub>2</sub>/90% N<sub>2</sub>) environments were applied to the non-catalytic as well as catalytic HTL treatments with two forms of RM catalysts: RM reduced at 500 °C (RRM) and nickel-supported RM (Ni/RM). Under nitrogen, ethylene and reducing environments, the biocrude yield increased by the following trend: No Catalyst < RRM < Ni/RM. The Ni/RM catalyst produced the highest biocrude yield (37 wt.%) in an ethylene environment, generated the lowest total acid number (14 mg KOH/g) under inert atmosphere, and lowered sulfur (33–66%) and oxygen (18–30%) from biocrude products irrespective of environments. The RRM catalyst maximized the biocrude carbon content (61 wt.%) under a reducing environment and minimized the heavy metal and phosphorus transfer from the feedstock to biocrude in studied ambiances. The reducing environment facilitated mild hydrotreatment during HTL reaction in the presence of RRM catalyst. Among the non-catalytic experiments, the reducing atmosphere optimized carbon content (54.3 wt.%) and calorific value (28 MJ/kg) with minimum oxygen amount (27.2 wt.%) in biocrudes.

**Keywords:** hydrothermal liquefaction; algae; red mud; ethylene; reaction environment; catalyst; biocrude



**Citation:** Rahman, T.; Jahromi, H.; Roy, P.; Adhikari, S.; Feyzbar-Khalkhali-Nejad, F.; Oh, T.-S.; Wang, Q.; Higgins, B.T. Influence of Red Mud Catalyst and Reaction Atmosphere on Hydrothermal Liquefaction of Algae. *Energies* **2023**, *16*, 491. <https://doi.org/10.3390/en16010491>

Academic Editor: Marcin Dębowski

Received: 29 October 2022

Revised: 16 December 2022

Accepted: 22 December 2022

Published: 2 January 2023



**Copyright:** © 2023 by the authors. Licensee MDPI, Basel, Switzerland. This article is an open access article distributed under the terms and conditions of the Creative Commons Attribution (CC BY) license (<https://creativecommons.org/licenses/by/4.0/>).

## 1. Introduction

Hydrothermal liquefaction (HTL) is a widely studied conversion technology for biomass liquefaction where the conversion of biomass takes place under sub- or super-critical condition of water, acting it as both reactant and catalyst and produces liquid (also known as biocrude), aqueous, solid, and gaseous products ([1,2] figure). The advantage of HTL process includes the total utilization of all three products for chemicals, advanced carbon materials and transportation fuel [3]. Moreover, pretreatment of feedstocks can improve the HTL biocrude yield [4]. Algae are a diverse group of aquatic organisms, gained worldwide attention for renewable biofuel production by HTL process as drying stage can be avoided [5]. Moreover, high biofuel precursor (lipid, starch) content, the ability to grow in non-arable land or in wastewater with high growth rates, have proved the potential of algae feedstock in biofuel production [6–8]. Therefore, several researchers have explored the HTL technology for various algae conversion. Recently, Jazie et al. have maximized algae (*F. vesiculosus*) derived biocrude oil yield by 27.6%, utilizing 15% of H $\beta$  zeolite catalyst loading with residence time of 20 min and at reaction temperature of 300 °C [9]. Kandasamy et al. have found enhanced biocrude yield (33%) from HTL conversion of *Spirulina platensis* algae at lower temperature (250 °C) with feedstock (*Spirulina platensis*) biochar supported CeO<sub>2</sub> catalyst [10]. Xia et al. have produced 10% higher

biocrude yield from co-liquefaction of rice straw and algae (*Nannochloropsis*) using alkali catalyst ( $K_2CO_3$ ) in glycerol-water solvent compared to pure rice straw feedstock [11]. Norouzi et al. have utilized functionalized graphene oxide/polyurethane composite as catalyst for HTL of *Cladophora glomerata* and effectively repealed the undesired chemicals formation in biocrudes [12]. Yu et al. produced biocrude from HTL conversion of algae grown on brackish dairy wastewater and valorized the HTL solid byproduct (hydrochar) as renewable anode material for lithium-ion batteries [13]. Guo et al. have showed that the addition of dichloromethane solvent induced about 9 wt.% higher biocrude yields of microalgae *Chlorella vulgaris*, compared to non-solvent separation technique [14]. Biswas et al. have explored the co-hydrothermal liquefaction of Prot lignin and *Sargassum tenerrium* macroalgae in water, ethanol, and water-ethanol solvent mixture and found a 7:3 ratio of lignin:macroalgae feedstock under water-ethanol solvent mixture could maximize the biocrude yield [15]. To reduce the algae production cost, researchers around the world adopted various strategies. Chen et al. have reused the aqueous HTL by product from *Chlorella* sp. algae conversion to grow the feedstock [16]. Mishra et al. utilized domestic wastewater as growth medium of *Monoraphidium* sp. algae and later blended the algae with domestic wastewater derived sewage sludge for co-liquefaction [17]. In a similar co-HTL study, Islam et al. increased the fecal sludge portion in co-liquefaction of algae and sludge mixture and noticed that the blend of 25% microalgae: 75% fecal sludge could produce the highest biocrude yield with lighter hydrocarbon content [18]. Kim and Lee incorporated a transparent low-density polyethylene film-based floating photobioreactor to culture *Tetraselmis* sp. microalga strain in the ocean [19]. Fon Sing et al. also determined that *Tetraselmis* sp. can maintain high growth rate under various salinity levels ranging from saline to hypersaline conditions [20]. For low production cost and high growth rate, *Tetraselmis* sp. can be a promising algal feedstock for HTL biocrude production.

The HTL biocrude derived from algae has a high viscosity, high oxygen and nitrogen, and low heating value. Catalytic HTL treatment is a suitable option to upgrade this product. The bauxite plant residue called red mud (RM) can be used as an inexpensive catalyst by modifying its properties. The heterogeneity of this industrial waste with high iron content can work as a liquefaction catalyst since iron is known to react with hot compressed water or steam and produce in situ hydrogen to react with the organic fractions of feedstock [21]. Red mud has been employed as catalyst support due to its low cost, strong stability, high surface area, sintering resistance, and resistance to poisoning [22]. The catalytic effects of red mud were already studied in HTL conversion of different feedstocks such as algae (*Spirulina platensis*), lignocellulosic biomass (oak wood), sewage sludge [23–25]. In separate studies, nickel (Ni)-based catalysts supported by  $Al_2O_3$  have been used for hydrotreatment of the algal biocrude oil, which removed sulfur, nitrogen and oxygen heteroatoms from oil with increased higher heating value (HHV) [26,27]. Red mud supported Ni (Ni/RM) catalyst successfully utilized for hydrodeoxygenation of pyrolysis oil and hydrogen production by ammonia decomposition [22,28]. Due to the perceived potential of Ni/RM, it is being tested for HTL process as well. The reaction atmosphere is an important operating parameter that can affect the distributions of HTL products. Peng et al. found that under  $CO$ ,  $H_2$  and  $N_2$  gaseous reaction environments biocrude yield from cornstalk followed this trend:  $CO > H_2 > N_2$  [29]. Wang et al. also used  $H_2$ , syngas ( $H_2$ : 68.1%,  $CO$ : 30.1%,  $C1-C4$ : 0.9% and  $CO_2$ : 0.9%), Ar and  $CO$  gases in HTL conversion of sawdust feedstock and mentioned that  $H_2$  gas generated more biocrude yield than syngas, Ar, and  $CO$  [30]. Yang et al. found out that Ni/REHY (REHY, Y zeolite exchanged with rare earth) catalyst achieved further deoxygenation and desulfurization of algae (*Dunaleilla salina*) derived HTL biocrude product under hydrogen gas [31]. However, understanding the effect of reaction environment over catalytic and non-catalytic HTL conversion of any algal feedstock is still rare.

This work aims to investigate the effect of inert, ethylene, reducing and oxidizing reaction environments over non-catalytic as well as catalytic HTL treatment of "*Tetraselmis* sp." algae strain. Our previous work showed the superiority of ethylene reaction atmosphere

with reduced red mud (RRM) catalysts over inert(nitrogen) conditions by increased yield and stability of municipal sewage sludge derived HTL biocrude [32]. Current study is designed to assess the influence of four different reaction atmospheres over HTL process of highly productive *Tetraselmis* sp. algae strain with the reduced red mud (RRM) and Ni metal on RM support (Ni/RM) catalysts. The hypothesis of this study is that the RRM and Ni/RM will enhance biocrude yield and carbon recovery from *Tetraselmis* feedstock. It is also expected that the RM catalysts under reducing environment could promote mild hydrogenation of *Tetraselmis* derived biocrude during the HTL reactions whereas the oxidizing environment may lead to oxidation of reactive functional groups in biocrude. Thus, the goal is to enhance biocrude production from highly productive algal feedstock with improved quality, which can be further upgraded via hydrotreatment.

## 2. Materials and Methods

### 2.1. Material

*Tetraselmis* sp. microalga was purchased from Reed Mariculture Inc. (Campbell, California, USA). Red mud (RM) was obtained from Almatix Burnside, Inc. (Gonzales, Louisiana, USA). Airgas Inc. (Opelika, Alabama, USA) supplied high purity nitrogen, ethylene, and a gas mixture of 10% H<sub>2</sub>/90% N<sub>2</sub> and 10% O<sub>2</sub>/90% N<sub>2</sub> denoted as reducing and oxidizing reaction ambience, respectively, in this study. Nickel (II) nitrate hexahydrate (99 wt.% crystalline) was purchased from Sigma–Aldrich (St. Louis, MO, USA) and was used as received.

### 2.2. Feedstock Characterization

For feedstock characterization, the algae samples were dried at 105 °C for 24 h, and a planetary ball mill (MSK-SFM-1S, MTI Corporation, Richmond, CA, USA) was used to grind the dried samples for uniform size. The EPA 1684 method was followed to measure the total solid content. The ash content was quantified using ASTM E1755 method. Biochemical composition of *Tetraselmis* sp. strain was provided by the supplier. The elemental analysis (CHNS/O) was performed according to the ASTM D5373-02 method in Vario MICRO cube, Elementar (New York, NY, USA). The higher heating value (HHV) of dried algae samples was determined using a unified correlation (Equation (1)) based on elemental analysis, proposed by Channiwala et al.

$$\text{HHV} = 0.3491 \cdot C + 1.1783 \cdot H + 0.1005 \cdot S - 0.1034 \cdot O - 0.015 \cdot N - 0.0211 \cdot A \quad (1)$$

where, C, H, O, N, S and A represents carbon, hydrogen, oxygen, nitrogen, sulfur, and ash contents of material, respectively, expressed in mass percentages on dry basis [33].

### 2.3. Catalyst Preparation

The RRM catalyst was prepared according to our previous work [32]. The as-received RM was calcined at 575 °C for four hours without any pretreatment and then sieved to obtain the particle size between 106–595 µm. The sieved calcined RM was reduced at 500 °C temperature. The reduction temperatures for RM were based on TG-TPR (Thermogravimetric-temperature programmed reduction) profile. For RM reduction, a gas mixture of 10% H<sub>2</sub> and 90% N<sub>2</sub> was used for six hours at the predetermined temperature. Incipient wetness impregnation method was used to prepare Ni/RM catalysts with nickel nitrate hexahydrate (Ni(NO<sub>3</sub>)<sub>2</sub>·6H<sub>2</sub>O) salt. The details of Ni/RM catalyst preparation and characterization such as TG-TPR (Thermogravimetric-temperature programmed reduction) analysis can be found in published document elsewhere [28]. In brief, 20 g of calcined RM with 106–595 µm particle size was mixed with 350 mL deionized water. To this slurry, a calculated amount of Ni(NO<sub>3</sub>)<sub>2</sub>·6H<sub>2</sub>O salt was added to give 10% Ni loading in the final catalyst. The metallic salts mixed with calcined red mud slurry were stirred at 80 °C for 4 h to obtain a thick mixture. The mixture was then dried at 105 °C overnight to obtain catalyst precursors. The catalyst precursor was calcined for 5 h in air at 620 °C in a muffle furnace (Thermo Scientific, Inc., Waltham, MA, USA). Then, the calcined material was reduced

for 6 h at 500 °C using a reducing gas mixture of 10% H<sub>2</sub> and 90% N<sub>2</sub> to obtain the final catalyst.

#### 2.4. Catalyst Characterization

Inductively coupled plasma-optical emission spectrometry (ICP-OES), X-ray diffraction (XRD) techniques, and surface analyzer methods were used to characterize the catalysts. The Soil, Plant, and Water Laboratory (University of Georgia, Athens, USA) performed ICP-OES analysis. XRD analysis was performed by the method discussed in our previous work [34]. Briefly, a bench-top powder X-ray diffraction system (AXRD, Proto Manufacturing, Taylor, MI, USA) was utilized from 20° to 100° (2θ) with 2 s of dwell time and 0.014° of Δ2θ at 30 mA and 40 kV with CuKα radiation (λ = 1.5418 Å). An Autosorb-iQ (Quantachrome Instruments, Boynton Beach, FL, USA) measured the specific surface area of the catalysts by BET (Brunauer–Emmett–Teller) equation using N<sub>2</sub>-adsorption–desorption isotherm in an adsorption analyzer. The physisorption macro steps can be found in our previous work [35].

#### 2.5. Experimental Setup and Procedure

A high-pressure, high-temperature reactor from Parr Instrument Company (Model 4578, Moline, IL, USA) was used for HTL experiments. The reactor setup was the same as our previous work [32]. The reactor has 1.8 L vessel, PID controlled electrical heating unit, controllable agitator, pressure gauge, and J-type thermocouple to monitor the temperature inside the reactor. For all reaction environments (nitrogen, ethylene, reducing and oxidizing), the HTL experiments were performed at a reaction temperature of 275 °C, agitator speed of 550 rpm and a residence time of 60 min. For each HTL experiment, 450 g as-received *Tetraselmis* sp. (with 18–19% solid content) was loaded into the reactor. For all catalytic HTL experiments, catalyst:feedstock loading was fixed at 1:10 on basis of solid content of feedstock (i.e., ~8 g catalyst per 450 g as-received feedstock). The reactor was purged with desired gas (nitrogen, ethylene, 10% H<sub>2</sub>/90% N<sub>2</sub> and 10% O<sub>2</sub>/90% N<sub>2</sub>) three times to remove air from the reactor headspace before pressurizing with it to an initial pressure of 200 psi (1.38 MPa). The reactor was then heated to the desired temperature at the heating rate of ~3 °C/min. After holding the reactor at 275 °C temperature for 1 h, the heater was removed, and the reactor was cooled to a room temperature by running cold water in the internal cooling coil. The products (gas, solid, aqueous phase, and biocrude) were separated as described in Section 2.6. All experiments were performed in duplicates.

#### 2.6. Product Separation

After cooling down the reactor to room temperature, the gas was analyzed. Then, the remaining gaseous products were vented and the reactor was opened to recover the liquid and solid products. The content in the reactor was poured into a large flask, and the weight was recorded. The aqueous phase and biocrude mixed solid remaining (char) were separated by gravity after the HTL reaction. The aqueous product was separated by decantation and heavier solid char with biocrude remained at the bottom layer. Then, the bottom layer was filtered through Whatman No.50 filter paper (particle filtration size of 2.7 μm) for further separation of the solid from the organic phase. Then, the remaining solids on the filter paper were washed with methanol (MEOH). The weight of all liquids (aqueous and organic phases) was recorded for mass balance. The MEOH was separated from the biocrude using an IKA rotary evaporator at 85 °C and 230 mbar vacuum pressure to obtain MEOH extracted bio-oil, which is termed as “biocrude oil” throughout the paper.

#### 2.7. Product Analysis

The gas products were analyzed using a micro-GC (Agilent 3000A, Agilent, Santa Clara, CA, USA) as discussed elsewhere [32]. The Agilent 3000 A Micro GC is equipped with three modules: a 10 m Molsieve 5A (MS) column and two 10 m porous polymer (PPU) columns. Each module had a thermal conductivity detector. The instrument can split the

sample into three streams. Each stream would go to one of these modules. MS column was used to analyze hydrogen, methane, and carbon monoxide, while carbon dioxide and ethylene hydrocarbons were analyzed on the PPU columns simultaneously. Argon and helium were used as carrier gases for MS column and PPU column, respectively. The gas composition analysis was performed in triplicates.

The mass of the gaseous product was calculated by using Equation (2).

$$W_g = \sum x_i \cdot MW_i \cdot n_{tot} \quad (2)$$

where  $W_g$  is the total mass of gaseous product (g),  $x_i$  is the mole fraction of gas  $i$ ,  $MW_i$  is the molecular weight of gas  $i$  (g/mole), and  $n_{tot}$  is the total number of moles of gas product.

In the case of ethylene, reducing, oxidizing HTL experiments, ethylene ( $C_2H_4$ ), hydrogen ( $H_2$ ), oxygen ( $O_2$ ) consumption was estimated using Equation (3).

$$Gas\ consumption \left( \frac{(mole\ of\ gas)}{(kg\ Algae)} \right) = (n_{i\ gas} - x_{f\ gas} \cdot n_{f\ tot}) \times \frac{1}{mass\ of\ algae} \times \frac{1000\ g}{1\ kg} \quad (3)$$

where  $n_{i\ gas}$  is the initial number of moles of ethylene, hydrogen, or oxygen,  $x_{f\ gas}$  is the final mole fraction of ethylene, hydrogen, and oxygen.  $n_{f\ tot}$  is the total number of moles of gas at the end of the experiment [32]. The yield of biocrude and solid product were calculated on dry-ash free basis using Equations (4) and (5), respectively [36]. The remaining product fraction was regarded as “balance” and calculated using Equation (6).

$$Y_{biocrude}(\%) = \frac{w_b}{w_f - w_m - w_a} \times 100 \quad (4)$$

$$Y_{solid}(\%) = \frac{w_s - w_c}{w_f - w_m - w_a} \times 100 \quad (5)$$

$$Y_{balance}(\%) = 100 - Y_{biocrude} - Y_{solid} \quad (6)$$

where  $w_f$  is the mass of *Tetraselmis* sp. algae feedstock (g),  $w_m$  and  $w_a$  are the mass of moisture and ash content of feedstock (g), respectively,  $w_b$  is the mass of the biocrude product (g),  $w_s$  is the weight of total solid residues (g), and  $w_c$  is the weight of catalyst (g).

The elemental analysis was performed on each sample using an elemental analyzer (Vario MICRO, Elementar, NY, USA) according to ASTM D5373-02. Effects and interactions of catalysts and reaction environments on biocrude yield, carbon, sulfur, ash and oxygen content were analyzed by the two-way analysis of variance (ANOVA) at 0.05 significance level followed by Tukey HSD test, using statistical programming software R [37]. V20 Volumetric Karl Fischer Titrator (Mettler Toledo, Columbus, OH, USA), was used in this study to measure the water content of the algal biocrudes. The higher heating value (HHV) of biocrude was determined using Equation (1). The total acid number (TAN) of each sample was determined through titration according to ASTM D664-07 using a Mettler Toledo T50 Titrator. Thermogravimetric analysis (TGA) of biocrude was performed by using a Shimadzu TGA-50 (Shimadzu, Japan) under nitrogen atmosphere (flow rate: 20 mL/min) with heating rate of 10 °C/min from room temperature up to 800 °C [38]. The chemical composition of each biocrude sample was subsequently analyzed by Fourier transform infrared (FTIR) and nuclear magnetic resonance (NMR) spectroscopy analyses. The FTIR of biocrudes was performed by using Thermo Nicolet iS10 (Thermo Scientific, Waltham, MA, USA). The samples were analyzed for 34 scans over a range of 400–4000  $cm^{-1}$  wavenumbers. Samples for NMR spectroscopy containing 15 mg of oil in 1 mL of ethanol-d<sub>6</sub> (99.9 atom% D) (Acros organic, Switzerland) were prepared in 5 mm 535-PP NMR tubes (Wilmad-LabGlass, Vineland, NJ, USA). <sup>13</sup>C spectra were collected using a Bruker 500 MHz spectrometer equipped with a broadband nitrogen-cooled prodigy probe. The spectra were referenced to ethanol-d<sub>6</sub> ( $C_2D_6O$ ,  $\delta^{13}C = 56.96$  and 17.31 ppm) and processed in Bruker Topspin software (4.1.3 version). The chemical composition of biocrude samples was also analyzed by an Agilent Technologies 7890A Gas Chromatograph (GC)

System outfitted with a 7683B Series Injector and 5975C Inert Mass Selective Detector (MSD) with Triple-Axis Detector. In brief, 30 m × 250 μm × 0.25 μm DB-35MS column was used in GC-MS to analyze the product. During analysis, the GC oven was heated to an initial temperature of 50 °C and held for 2 min and then ramped at a heating rate of 5 °C/min to a final temperature of 280 °C and holding time of 15 min. The chemical structures identified by the National Institute of Standards and Technology (NIST) MS Library of the GC-MS were then semi-quantified based on their peak area percentage.

The aqueous phase analysis followed the procedure as discussed in the published document elsewhere [32]. Total organic carbon (TOC), total nitrogen (TN) with specific species distribution (ammonium (NH<sub>4</sub><sup>+</sup>-N), nitrate (NO<sub>3</sub><sup>-</sup>-N), organic nitrogen (Org-N)), chemical oxygen demand (COD), and pH, were measured to characterize the aqueous products. The TOC and TN were measured by a TOC/TN analyzer (TOC-L, Shimadzu, Kyoto, Japan). A Prominence Liquid Chromatography (LC) system coupled with a conductivity detector (Shimadzu, Japan) was used to analyze concentrations of ammonium (NH<sub>4</sub><sup>+</sup>-N) and nitrate (NO<sub>3</sub><sup>-</sup>-N) in digestate samples. The detailed procedure can be found elsewhere [39]. Briefly, A Dionex IonPac CS12 column (4 × 250 mm, Thermoscientific, Sunnyvale, CA, USA) and a Dionex IonPac AS22 column (4 × 250 mm) with suppression (Dionex CERS 500 4 mm and Dionex AERS 500 4 mm, respectively) were used for ion separation. Acidic eluent (20 mM methane sulfonic acid) was used on the CS12 column, and basic eluent (4.5 mM sodium carbonate and 1.4 mM sodium bicarbonate solution) was used on the AS22 column. The amount of organic nitrogen (Org-N) was calculated by the difference of total nitrogen and inorganic nitrogen (the sum of NH<sub>4</sub><sup>+</sup>-N and NO<sub>3</sub><sup>-</sup>-N). The COD was determined using a COD assay kit (HACH, Loveland, Colorado, USA) and a spectrometer (DR900, HACH, Loveland, CO, USA). The detailed procedure can be found in a published document [40]. The pH of the solution was measured using a pH meter (pH510, Oakton, Vernon Hills, IL, USA).

### 3. Results and Discussion

#### 3.1. Feedstock Characterization

The physicochemical properties of the chosen algae feedstock (*Tetraselmis* sp.) were studied by elemental composition analysis (CHNS/O), higher heating value (HHV), ash content and the biochemical composition. The characterization result of *Tetraselmis* sp. along with other algae strains on dry basis is presented in Table 1. The carbon content and HHV of *Tetraselmis* sp. was lower than other strains, which is supported by previous *Tetraselmis* reports [41,42]. The biochemical composition of the algae varied widely with the strain. *Tetraselmis* strain has high protein content similar to *Nannochloropsis* strain [43]. The ash content of *Tetraselmis* sp. was also in agreement with the previous work. The saline growth culture for this alga might be responsible for ash content [41].

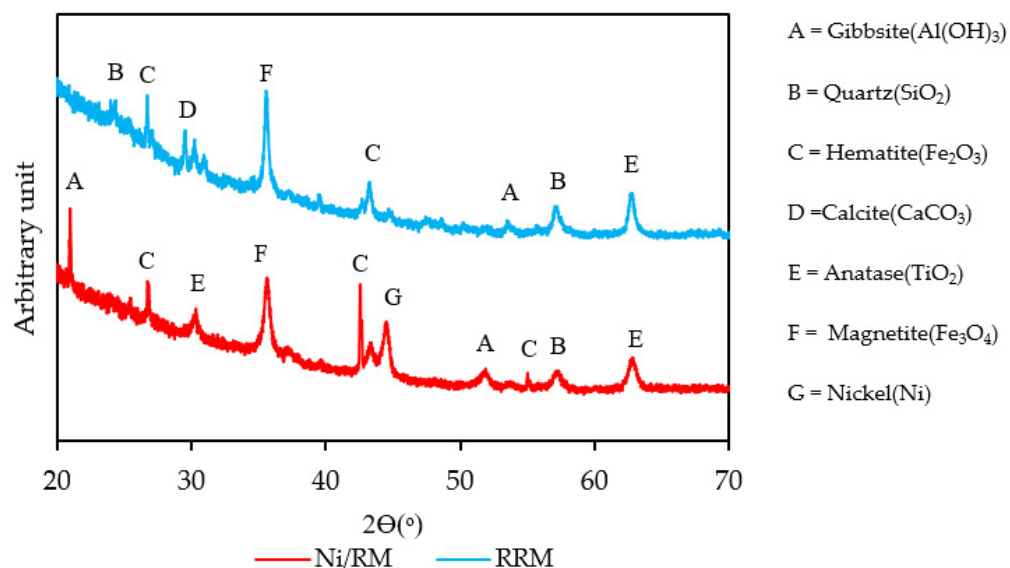
#### 3.2. Catalyst Characterization

Due to difficulties in separation of catalysts from char, only fresh catalysts were analyzed. Figure 1 illustrates the XRD analysis of RRM and Ni/RM catalysts. Metal oxides such as gibbsite (Al(OH)<sub>3</sub>), quartz(SiO<sub>2</sub>), hematite(Fe<sub>2</sub>O<sub>3</sub>), calcite(CaCO<sub>3</sub>), anatase(TiO<sub>2</sub>) and magnetite(Fe<sub>3</sub>O<sub>4</sub>) were detected in these RM based catalysts. Major peaks of iron (hematite, magnetite) were detected by XRD analysis in both catalysts. ICP-OES analysis (Table S1, Supplementary Material) also determined a significant amount of Fe metal in RRM and Ni/RM catalysts where RRM contained 11.8% more iron than Ni/RM catalyst. The prominent XRD peak of nickel (Ni) in Ni/RM catalyst indicated the successful incorporation of this transition metal on RM support. 10.5 wt.%(104,802 ppm) of Ni metal was detected by ICP-OES analysis in Ni/RM catalyst, which was very close to the desired Ni loading. However, no significant difference was observed in BET surface area (Table S2) of Ni/RM (22.4 m<sup>2</sup>/g) and RRM (21.9 m<sup>2</sup>/g) catalysts.

**Table 1.** Characterization of *Tetraselmis* sp. feedstock and comparison with other algae strains [43].

	<i>Tetraselmis</i>	<i>Nannochloropsis</i>	<i>Pavlova</i>	<i>Isochrysis</i>
Proximate Analysis <sup>a</sup> (wt.%)				
Moisture	82.00 ± 1.20	68.88 ± 1.24	75.80 ± 0.42	73.93 ± 1.44
Ash	2.60 ± 0.10	3.42 ± 0.38	3.47 ± 0.33	3.39 ± 0.29
Volatile content	13.20 ± 0.30	22.51 ± 1.28	17.74 ± 0.77	18.20 ± 1.01
Elemental Composition <sup>b</sup> (wt.%)				
C	32.20 ± 0.31	56.83 ± 0.33	54.34 ± 1.36	55.76 ± 1.14
H	5.13 ± 0.23	9.32 ± 0.06	8.69 ± 0.41	8.70 ± 0.34
N	4.42 ± 0.05	10.13 ± 0.06	8.67 ± 0.21	7.96 ± 0.06
S	0.79 ± 0.11	0.37 ± 0.19	0.82 ± 0.09	0.62 ± 0.10
Ash	15.00 ± 0.20	3.42 ± 0.38	3.47 ± 0.33	3.39 ± 0.29
O <sup>c</sup>	42.46 ± 0.90	19.93 ± 0.26	24.01 ± 2.07	23.57 ± 1.65
H/C ratio	1.90	1.96	1.91	1.87
HHV <sup>b</sup> (MJ/kg)	12.60 ± 0.20	24.02 ± 0.07	22.69 ± 0.07	22.97 ± 0.02
Biochemical Composition <sup>b</sup> (wt.%)				
Protein	63.00	62.79	46.94	44.36
Lipid	11.00	18.12	13.88	18.98
Carbohydrate	11.00	8.92	28.00	25.46

<sup>a</sup> as received basis, <sup>b</sup> dry basis, <sup>c</sup> by difference.

**Figure 1.** XRD pattern of RRM and Ni/RM catalysts.

### 3.3. HTL Products Characterization

#### 3.3.1. Products Yield Distribution

Figure 2 demonstrated the product distribution (on dry-ash free basis) for catalytic and non-catalytic HTL experiments of *Tetraselmis* under four reaction environments. Without the use of catalyst, the inert (nitrogen) environment generated the highest biocrude yield by 22.8 wt.% where the reducing environment produced the lowest biocrude yield by 17 wt.%. The trend of biocrude yield in non-catalytic reactions under studied reaction environments was as follows: nitrogen > oxidizing > ethylene > reducing. The biocrude yield of this study was lower compared to other *Tetraselmis* HTL biocrude studies where biocrude products

were extracted by dichloromethane (DCM) solvent [41,44]. The increased biocrude yield by DCM solvent from *Chlorella vulgaris* microalgae and municipal sewage sludge feedstock was observed in previous HTL works [14,45]. The use of MEOH instead of DCM, for biocrude separation was the reason to obtain lower yield from *Tetraselmis* feedstock in the current work. From our previous work with municipal sewage sludge liquefaction, it was found that the dichloromethane (DCM) certainly enhanced the biocrude yield but the hydrotreatment of DCM-extracted biocrude was affected by catalyst deactivation, polymerization of biocrude, and equipment corrosion. The high chloride content in DCM-extracted biocrude was mainly responsible for these issues. To avoid the complication in downstream upgrading (hydrotreatment) stage, we incorporated MEOH to extract biocrude from *Tetraselmis* feedstock [46]. Incorporation of catalyst has increased the biocrude yield in inert, ethylene and reducing ambiances. Except for oxidizing environment, biocrude yield enhanced by the following trend: no catalyst < RRM < Ni/RM. The influence of catalysts over biocrude yield was found statistically significant (d.f. = 2, F = 32.9,  $p = 0.000$ ) but there was no interaction between the environment and catalysts (Supplementary Materials, Table S3). The Ni/RM catalyst successfully maximized the biocrude yield up to 37.4 wt.% in ethylene environment which closely matched with *Tetraselmis* biocrude yield from HTL study by the Pacific Northwest National Laboratory, at higher temperature (350 °C) in inert environment [47]. According to Wang et al., Ni catalyst (Ni/SiO<sub>2</sub>-Al<sub>2</sub>O<sub>3</sub>) is able to reduce the activation energy for algae building blocks (protein and carbohydrate) conversion which could generate more biocrude with higher nitrogen and oxygen content [48]. In this study, the elemental analysis (Table 2) of biocrude showed that RRM catalyst has increased the nitrogen content of biocrude in four reaction environments where Ni/RM has the same effect under oxidizing ambience. This finding suggested that Ni/RM catalyst might facilitate the higher conversion of protein from *Tetraselmis* during HTL process compared to non-catalytic or RRM reactions in all four reaction ambiances. In addition, the Ni/RM catalyst appeared to catalyze deoxygenation reaction under reactive ambiances (ethylene, reducing, and oxidizing environments). The reducing reaction environment and Ni/RM catalyst combination produced almost 91% more biocrude products comparing to non-catalytic reaction in reducing environment. The hydrogenation ability of hydrogen gas could be a reason for higher feedstock conversion during HTL process [30]. In oxidizing reaction ambience, the biocrude yield was also increased by the catalysts compared to non-catalytic condition. Unlike other three reaction conditions, RRM catalyst promoted more biocrude production than Ni/RM under oxidizing environment.

**Table 2.** Physicochemical properties of *Tetraselmis* HTL biocrude.

		Nitrogen			Ethylene			Reducing			Oxidizing		
		No Catalyst	RRM	Ni/RM	No Catalyst	RRM	Ni/RM	No Catalyst	RRM	Ni/RM	No Catalyst	RRM	Ni/RM
Elemental Composition <sup>a</sup> (wt.%)	C	47.9 ± 0.6	61.0 ± 0.1	53.9 ± 0.5	48.9 ± 0.2	57.0 ± 0.3	58.2 ± 0.3	54.3 ± 1.0	61.0 ± 0.1	59.3 ± 0.3	52.5 ± 0.3	54.6 ± 0.6	60.2 ± 0.3
	H	10.3 ± 0.4	10.6 ± 0.2	10.2 ± 0.1	10.4 ± 0.2	10.6 ± 0.1	10.5 ± 0.3	10.2 ± 0.5	10.9 ± 0.1	11.2 ± 0.1	10.1 ± 0.6	10.4 ± 0.1	9.5 ± 0.8
	N	3.1 ± 0.1	4.4 ± 0.1	4.0 ± 0.1	3.1 ± 0.1	4.1 ± 0.1	4.2 ± 0.1	3.5 ± 0.1	4.5 ± 0.1	4.5 ± 0.1	3.5 ± 0.1	3.9 ± 0.1	4.4 ± 0.1
	S	0.4 ± 0.1	0.5 ± 0.1	0.2 ± 0.1	0.5 ± 0.1	0.6 ± 0.1	0.2 ± 0.1	0.3 ± 0.2	0.4 ± 0.1	0.2 ± 0.1	0.5 ± 0.3	0.6 ± 0.1	0.3 ± 0.1
	Ash	6.0 ± 0.1	4.9 ± 0.1	4.5 ± 0.0	5.3 ± 0.1	3.8 ± 0.0	4.4 ± 0.2	4.4 ± 0.1	3.9 ± 0.1	2.9 ± 0.1	5.6 ± 0.0	3.4 ± 0.1	4.5 ± 0.0
	O <sup>b</sup>	32.3 ± 1.3	18.8 ± 0.4	27.2 ± 0.7	31.8 ± 0.6	23.9 ± 0.3	22.5 ± 0.8	27.2 ± 1.9	19.4 ± 0.3	21.9 ± 0.7	27.7 ± 1.2	27.1 ± 0.9	21.2 ± 1.1
Water Content (wt.%)		16.0 ± 2.3	10.3 ± 1.7	19.3 ± 2.2	16.6 ± 2.1	12.6 ± 1.8	10.0 ± 0.9	14.7 ± 1.2	11.7 ± 1.6	12.3 ± 1.0	13.9 ± 2.3	14.4 ± 1.2	12.1 ± 0.7
HHV (MJ/kg)		25.4 ± 0.8	31.7 ± 0.3	27.9 ± 0.3	26.0 ± 0.3	29.8 ± 0.2	30.3 ± 0.6	28.0 ± 1.1	32.1 ± 0.2	31.5 ± 0.4	27.3 ± 0.9	28.4 ± 0.4	29.9 ± 1.1
TAN (mgKOH/g)		21.9 ± 0.1	27.3 ± 1.0	14.0 ± 0.1	18.9 ± 0.4	24.6 ± 0.3	27.5 ± 0.3	26.3 ± 0.1	28.5 ± 0.1	28.3 ± 0.4	24.4 ± 1.8	27.1 ± 0.2	30.0 ± 0.8
Heavy Metal and Phosphorus (ppm)	Co	37.9 ± 0.1	44.3 ± 0.5	16.7 ± 0.3	40.3 ± 0.7	65.0 ± 0.2	57.1 ± 0.3	22.4 ± 0.8	22.1 ± 0.4	71.2 ± 0.5	20.6 ± 0.2	50.1 ± 0.6	52.6 ± 0.1
	Cr	1.3 ± 0.2	1.5 ± 0.4	1.0 ± 0.6	1.5 ± 0.8	0.4 ± 0.0	0.6 ± 0.0	0.9 ± 0.0	3.7 ± 0.6	2.7 ± 0.7	0.2 ± 0.0	1.9 ± 0.3	1.4 ± 0.4
	Cu	13.1 ± 1.0	4.0 ± 0.5	8.7 ± 1.2	<0.5 ± 0.0	<0.5 ± 0.0	13.4 ± 1.1	4.0 ± 0.8	<0.5 ± 0.0	4.7 ± 0.3	<0.5 ± 0.0	<0.5 ± 0.0	14.6 ± 1.4
	Fe	1075.0 ± 2.3	2788.1 ± 1.4	3173.1 ± 0.5	1145.2 ± 0.7	3408.6 ± 1.3	3253.5 ± 1.6	854.1 ± 0.8	2405.3 ± 0.7	1518.9 ± 1.4	588.4 ± 0.7	1050.5 ± 0.5	2233.7 ± 0.3
	Mn	<2.5 ± 0.0	<2.5 ± 0.0	<2.5 ± 0.0	5.0 ± 1.0	5.0 ± 1.1	<2.5 ± 0.0	5.0 ± 1.0	5.0 ± 1.1	5.6 ± 1.7	9.6 ± 1.4	5.0 ± 1.0	<2.5 ± 0.0
	Ni	280.5 ± 1.2	15.5 ± 0.7	1448.7 ± 1.6	12.7 ± 1.0	87.4 ± 1.6	1113.2 ± 1.4	8.1 ± 1.1	6.8 ± 1.2	1938.2 ± 2.3	16.5 ± 1.1	16.1 ± 0.6	1540.1 ± 1.6
	P	37.5 ± 0.6	9.6 ± 1.0	32.0 ± 1.6	43.0 ± 0.9	6.1 ± 1.4	9.3 ± 0.6	160.4 ± 0.3	34.9 ± 1.0	535.4 ± 0.5	25.5 ± 0.4	2.5 ± 0.7	8.7 ± 0.4
	Zn	13.5 ± 1.1	5.9 ± 0.6	12.2 ± 0.8	<2.5 ± 0.0	<2.5 ± 0.0	8.9 ± 1.4	14.0 ± 0.6	<2.5 ± 0.0	9.0 ± 1.1	9.9 ± 0.6	<2.5 ± 0.0	9.8 ± 1.0

<sup>a</sup> dry basis, <sup>b</sup> by difference.

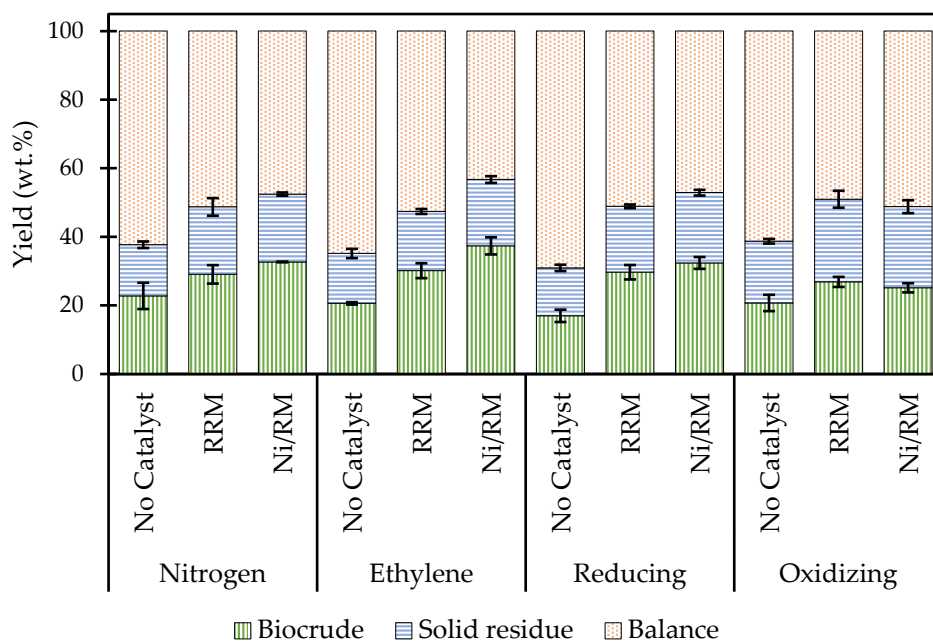


**Figure 2.** Yield distribution of *Tetraselmis* sp. (on dry-ash free basis) under different reaction environments and catalysts.

The solid residue increased with catalyst regardless of the reaction environment. Except oxidizing environment, the solid residue increasing trend was as follows: no catalyst < RRM < Ni/RM. The oxidizing environment increased the solid residue in both catalytic and non-catalytic reactions compared to other three reaction environments. The oxidizing atmosphere might promote oxidation of feedstock in HTL condition and raise the char yield. The RRM catalyst under oxidizing environment produced the highest solid residue by 24 wt.% whereas the lowest solid residue (14 wt.%) was found from no catalyst-reducing environment combination. The addition of Ni/RM catalyst led to 46% more solid residue production than non-catalytic reaction under reducing ambience.

### 3.3.2. Biocrude Characterization Physicochemical Properties

Table 2 shows the physicochemical properties of HTL biocrude from *Tetraselmis* algal feedstock. Due to MEOH solvent extraction, the *Tetraselmis* derived biocrude of this study has lower carbon and subsequently higher oxygen content compared to other report [42]. This phenomenon was already discussed in our previous work [46]. Among non-catalytic reactions, the reducing environment has maximized the carbon content with  $54.3 \pm 1.0$  wt.% and subsequently minimized the oxygen content ( $27.2 \pm 1.9$  wt.%). This result suggested that the reducing environment performed deoxygenation reaction without catalyst during HTL process. The ash and sulfur contents were also lowered by reducing ambience in non-catalytic reaction. Therefore, the HHV of the same biocrude subsequently increased by 10.6% compared to inert-no catalyst reaction derived biocrude. The hydrogen and nitrogen percentages in biocrudes remained almost the same in non-catalytic reactions under four reaction environments. Among catalytic and non-catalytic reactions, the inert environment-no catalyst combination generated highest ash (6 wt.%), oxygen percentage (32.3 wt.%) with the lowest carbon content of 47.9 wt.% in biocrude, which ultimately led to the minimum HHV of 25.4 MJ/kg. Ethylene reaction atmosphere reduced acidity (TAN) by 15–39% in non-catalytic biocrude compared to other non-catalytic experiments.

Prominent catalytic effects were observed in carbon, ash, sulfur, oxygen content and HHV of the biocrudes in all studied environments. Irrespective of reaction environments, both RRM and Ni/RM catalyst increased carbon and nitrogen percentage with reduced ash content in biocrudes compared to non-catalytic reactions. As a result, the oxygen

percentage was lowered in catalyst derived biocrudes with higher HHV. The interaction of reaction environment and catalyst over the carbon (d.f. = 6,  $F = 41.9$ ,  $p = 0.000$ ), ash (d.f. = 6,  $F = 28.2$ ,  $p = 0.000$ ) and oxygen (d.f. = 6,  $F = 12.7$ ,  $p = 0.000$ ) content of biocrude were statistically significant. The RRM catalyst in inert and reducing environments and Ni/RM catalyst in oxidizing environments were successful in maximizing carbon percentage in *Tetraselmis* biocrude by 61 wt.% and 60.2 wt.%, respectively. Increased carbon percentage was also found in HTL conversion of *Nannochloropsis salina* (*N. salina*) with Ni–Mo/ $\text{Al}_2\text{O}_3$  catalyst under  $\text{H}_2$  reaction ambience [49]. However, the catalytic HTL reactions raised the nitrogen content of the biocrudes. As discussed earlier (Section 3.3.1), the catalyst probably converted more protein compounds compared to non-catalytic reactions and increased the nitrogen content of the biocrudes. Incorporation of Ni metal on RM support has clearly favored deoxygenation reaction. The oxygen removal by Ni/RM followed this trend: inert < ethylene < reducing < oxidizing reaction environment. The low (1.35 wt.%) oxygen content in hydrotreated pyrolysis oil from pinyon-juniper was observed by Ni/RM catalyst at high pressure hydrogen (6.2 MPa initial pressure) [50]. In this study, the Ni/RM catalyst under reducing environment lowered oxygen percentage of biocrude by 20% compared to the Ni/RM-inert reactions under lower hydrogen pressure (1.37 MPa initial pressure). This finding suggested that Ni/RM catalyst might perform mild hydrodeoxygenation at lower hydrogen pressure of HTL process. Addition of Ni/RM catalyst also reduced the sulfur content of the biocrudes by 33–66% compared to non-catalytic and RRM catalytic reactions in four ambiances. This desulfurization of the biocrudes might occur due to the adsorption ability of Ni/RM catalyst [51]. The sulfur removal from biocrudes by catalyst was found to be statistically significant (d.f. = 2,  $F = 8.3$ ,  $p = 0.005$ ) without any interaction between environment and catalyst (Supplementary Material, Table S3).

The catalytic reactions increased TAN of *Tetraselmis* biocrude in all reaction environments, except inert atmosphere. Higher TAN was reported in HTL conversion of *Nannochloropsis* by Ni/ $\text{TiO}_2$  catalyst in inert atmosphere. Most probably, Ni/ $\text{TiO}_2$  catalyst promoted the hydrolysis of protein and lipids from algae in HTL process which generated more TAN increasing compounds such as carboxyl group enriched fatty acid, carboxylates, amino acid or phenolic compounds from amino acid conversion [48]. However, Ni/RM-inert reaction generated minimum acidity in the biocrude of this study. The presence of  $\text{TiO}_2$  with other metal oxides of  $\text{Al}(\text{OH})_3$ ,  $\text{SiO}_2$ ,  $\text{Fe}_2\text{O}_3$ ,  $\text{CaCO}_3$ , and  $\text{Fe}_3\text{O}_4$  in Ni/RM catalyst was confirmed by XRD analysis (Figure 1). Most probably, the mixed metal oxides of RM support affected the Ni/RM catalytic activity and suppressed the generation of TAN increasing compounds in *Tetraselmis* biocrude. Significant amount of water (10–19 wt.%) was detected in the biocrude products of this study. The utilization of MEOH solvent might be responsible for the excess water content of biocrudes. From ICP analysis, RRM catalyst was found to be more effective than Ni/RM catalyst to suppress the migration of heavy metals such as copper (Cu), zinc (Zn) and phosphorus (P) compounds to biocrudes irrespective of reaction environments. It is well established that treated or untreated RM can absorb heavy metals and phosphate from soil and water [52]. However, the effect of RM-based catalyst on metal content of HTL biocrude was rarely investigated. The lowest Cu (<0.50 ppm) and Zn (<2.50 ppm) contents were observed in biocrude from RRM-ethylene, reducing and oxidizing reaction environments. However, the minimum values of Cu, Zn or P from *Tetraselmis* biocrude were higher than conventional petroleum crude oil [53,54]. Significant leaching of iron (Fe) took place in catalytic reactions derived biocrude. The introduction of Ni metal on RM support also increased the Ni content in the biocrudes regardless of the reaction atmospheres. Under oxidizing environment, RRM catalyst reduced the iron migration to biocrude by 8–62% compared to other reaction conditions. The ethylene environment was successful in repealing the Ni leaching from Ni/RM catalyst to biocrude products by 30–74% compared to other three reaction environments.

### Thermogravimetric Analysis

Figure 3 presents the thermogravimetric analysis of biocrude products from catalytic and non-catalytic HTL conversion of *Tetraselmis* feedstock under nitrogen, ethylene, reducing and oxidizing reaction environments. Based on decomposition patterns, the TGA thermograms of the biocrudes were divided into three regions: 100–300 °C (referred to as light fraction), 300–550 °C (medium fraction), and 550–800 °C (heavy fraction). The biocrude products of this work contained 32–38 wt.% light fraction, 28–36 wt.% medium fraction and 13–22 wt.% heavy fraction. Among all non-catalytic reactions, the reducing environment generated 1.2–9.2% higher light fraction in biocrude. Regardless of the reaction environment, incorporation of catalysts increased the decline of biocrude weight percentage or mass loss in both medium and heavy fraction regions of the TGA graphs compared to non-catalytic reactions. The decomposition peak at around 80 °C in biocrudes (Figure 3A) might be due to remaining water in that specific biocrude sample which was supported by the water content data from Table 2. The lowest heavy fraction was found in biocrude sample from non-catalytic reaction under oxidizing ambience. The Ni/RM catalyst increased the mass loss in heavy fraction region by 90% compared to non-catalytic reaction in oxidizing environment. The heavy fraction decomposition in oxidizing environment showed following trend: No Catalyst < RRM < Ni/RM. At 130 °C, the biocrude mass loss in oxidizing environment exhibited following trend: No Catalyst > RRM > Ni/RM. This finding suggested that non-catalytic reaction under oxidizing environment might favor gasoline range products in *Tetraselmis* biocrude. The Ni/RM-reducing environment combination decreased heavy fraction of biocrude by 12.4–30.8%—compared to other three reaction ambiances with same catalyst.

### FTIR Analysis

FTIR spectra of *Tetraselmis* biocrude are presented in Figure 4.

In Figure 4A, reducing environment without catalyst showed higher intensity in four regions of hydroxyl and phenolic groups (3050–3700  $\text{cm}^{-1}$ ), methylene groups (2800–3000  $\text{cm}^{-1}$ ) and in bands of 1300–1750  $\text{cm}^{-1}$  compared to the other three reaction ambiances. The sharp peaks of 2800–3000  $\text{cm}^{-1}$  band under reducing environment suggested strong presence of C-H stretching in biocrude [55]. The increased peak in 3050–3700  $\text{cm}^{-1}$  region under reducing environment might appear due to high biocrude TAN value as oxygen content was lower in biocrude [48]. Variation in region of 980–1080  $\text{cm}^{-1}$  might cause by the lowest aliphatic esters from oxidizing environment where reducing environment has generated the maximum amount.

From Figure 4B, the reduction in peak of 3050–3700  $\text{cm}^{-1}$ , might take place due to the decline of -OH group as minimum oxygen content was reported (Table 2) from RRM catalyst under inert environment. Both RRM and Ni/RM increased methylene groups (2800–3000  $\text{cm}^{-1}$ ) and the bands of 980–1080  $\text{cm}^{-1}$  and 1300–1750  $\text{cm}^{-1}$  which suggested that catalysts might promote nitrogen heteroatom under inert condition which was consistent with the increasing nitrogen content (Table 2) of the catalytic biocrudes [55].

In ethylene atmosphere (Figure 4C), the catalysts have promoted the methylene groups (2800–3000  $\text{cm}^{-1}$ ) compared to non-catalytic biocrude. The RRM catalyst produced a sharp peak at 980–1030  $\text{cm}^{-1}$  area which could be explained by the enhanced nitrogen content of the biocrude (Table 2).

In Figure 4D, lower intensity in 3050–3700  $\text{cm}^{-1}$  area suggested that RRM and Ni/RM catalysts effectively reduced -OH group in reducing environment. This finding was also supported by the elemental analysis of the biocrude products where oxygen content of RRM catalytic reactions derived biocrude under reducing environment was lower compared to no catalyst and Ni/RM conditions.

In oxidizing environment (Figure 4E), the suppressed peak of -OH group by Ni/RM catalyst was supported by the lower oxygen content of the same biocrude. The Ni/RM catalyst also generated sharper peak in methylene group (2800–3000  $\text{cm}^{-1}$ ) and in band

of 1300–1750  $\text{cm}^{-1}$ . The peaks from catalytic biocrudes in 980–1080  $\text{cm}^{-1}$  area, were close where RRM catalyst has shown little more intense peak compared to Ni/RM catalyst.

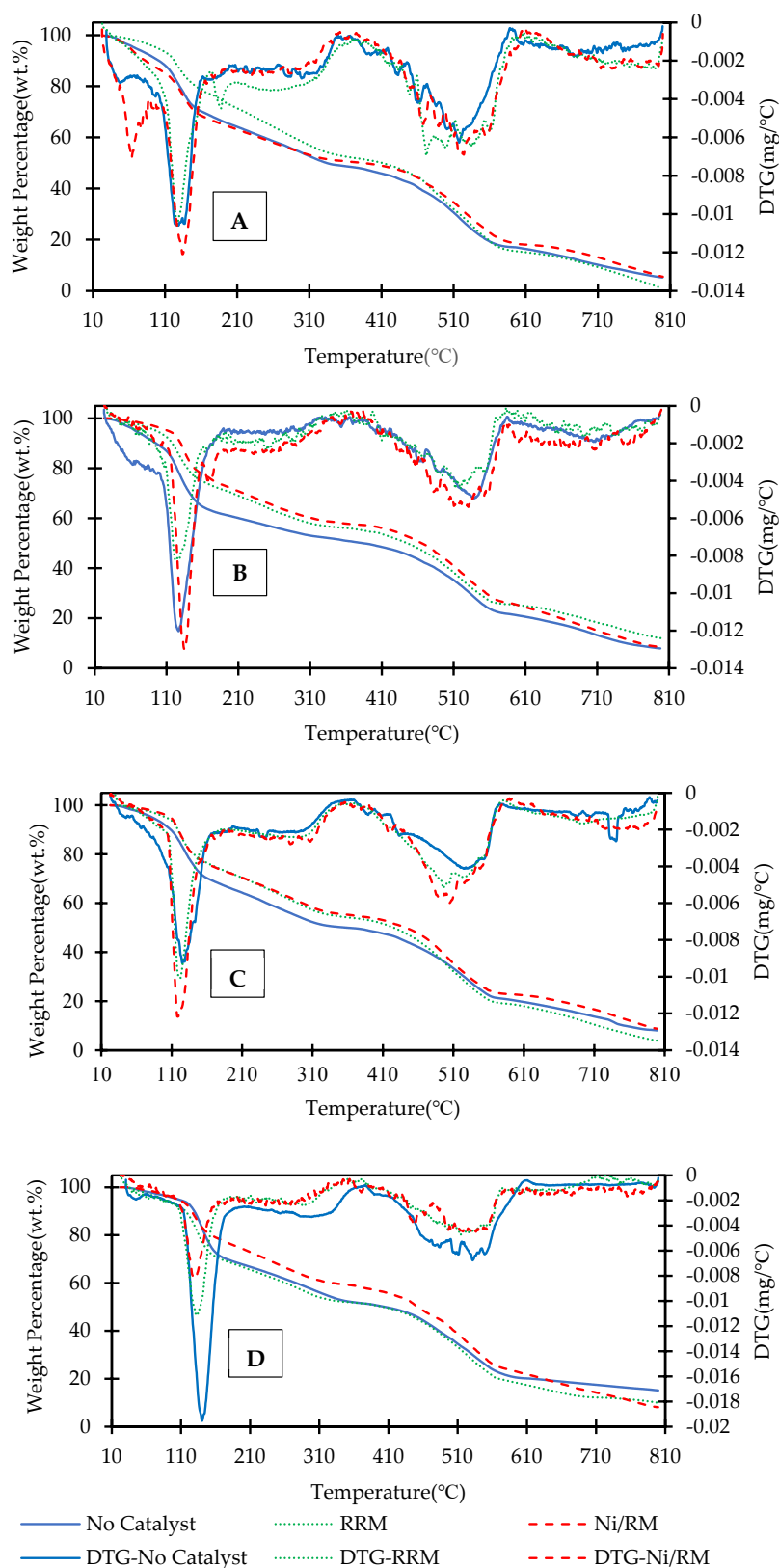


**Figure 3.** Thermogravimetric analysis of biocrude samples from non-catalytic and catalytic reactions: (A)—Nitrogen, (B)—Ethylene, (C)—Reducing and (D)—Oxidizing reaction environments.

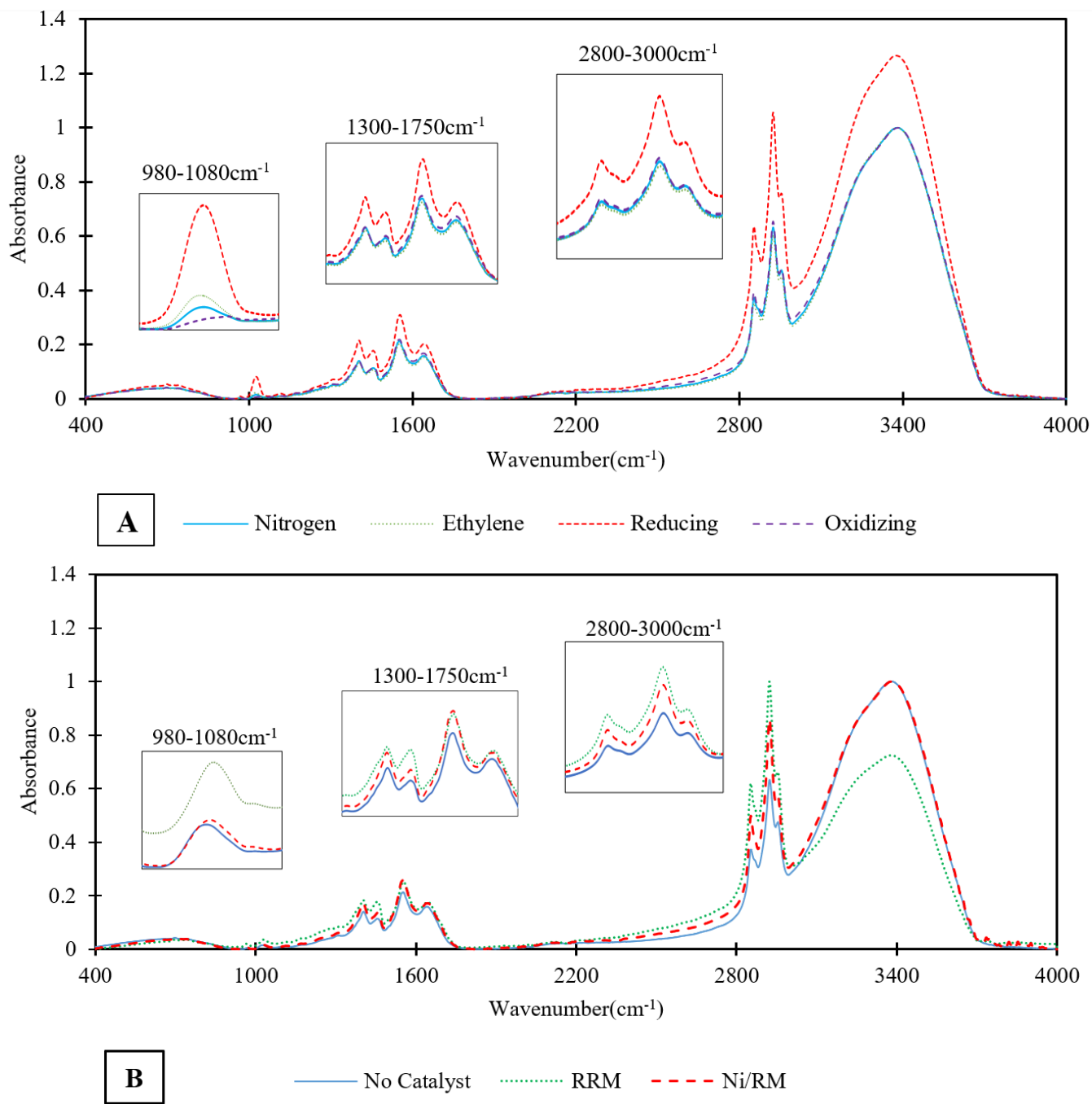
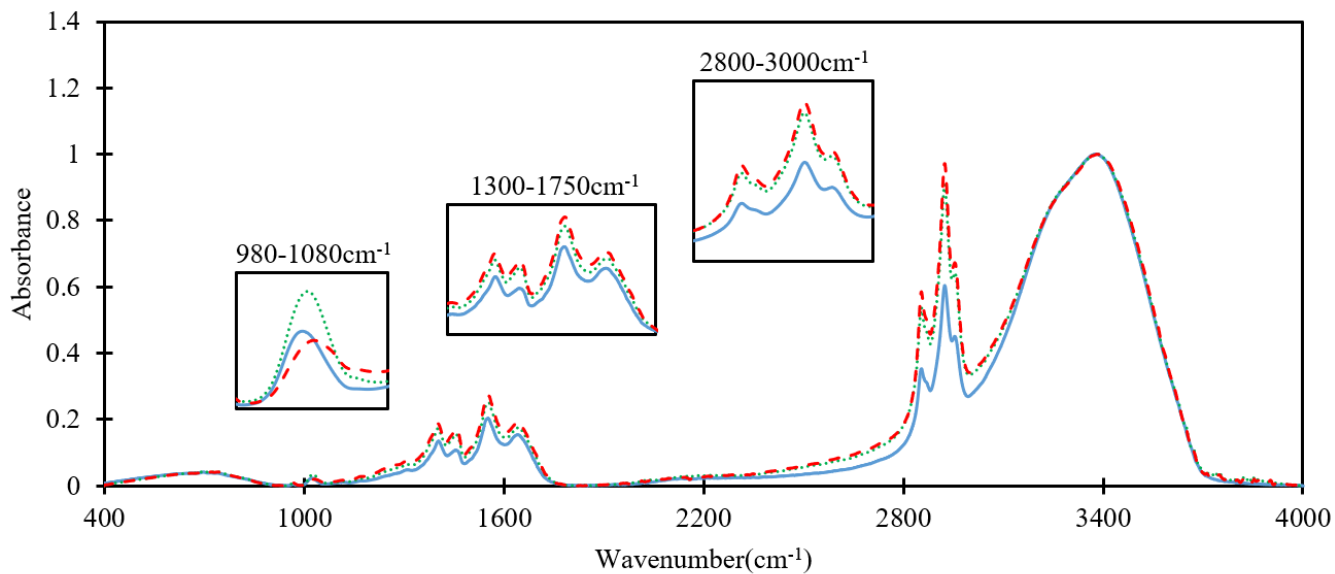
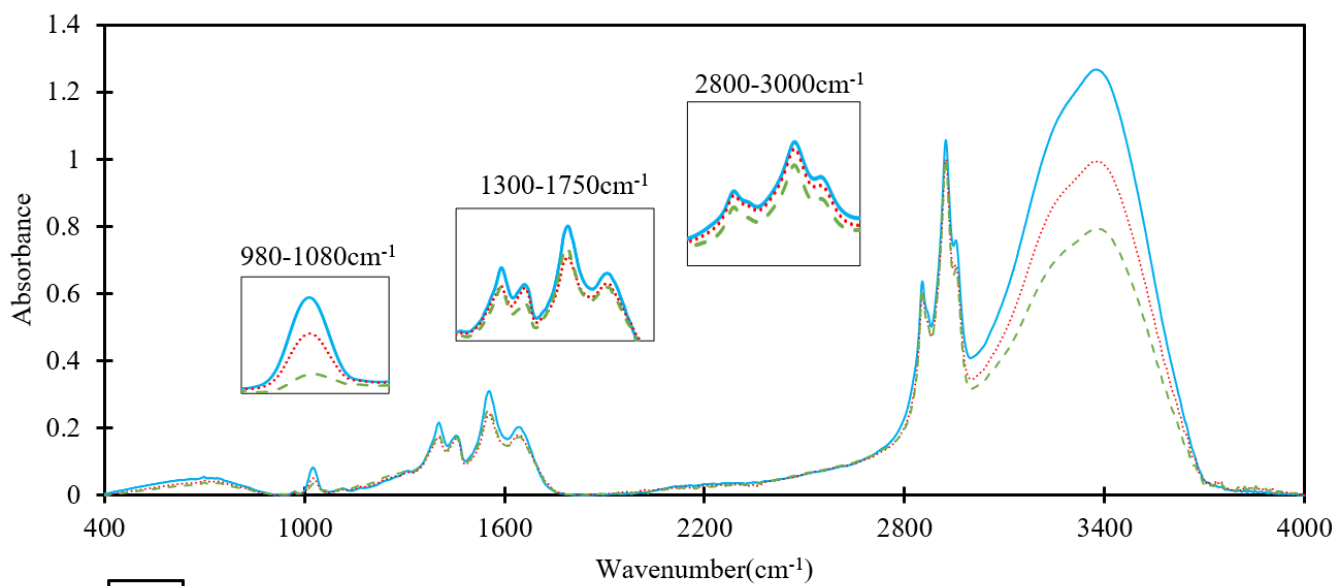


Figure 4. Cont.



**C**

— No Catalyst    ..... RRM    - - - Ni/RM



**D**

— No Catalyst    ..... Ni/RM    - - - RRM

Figure 4. Cont.

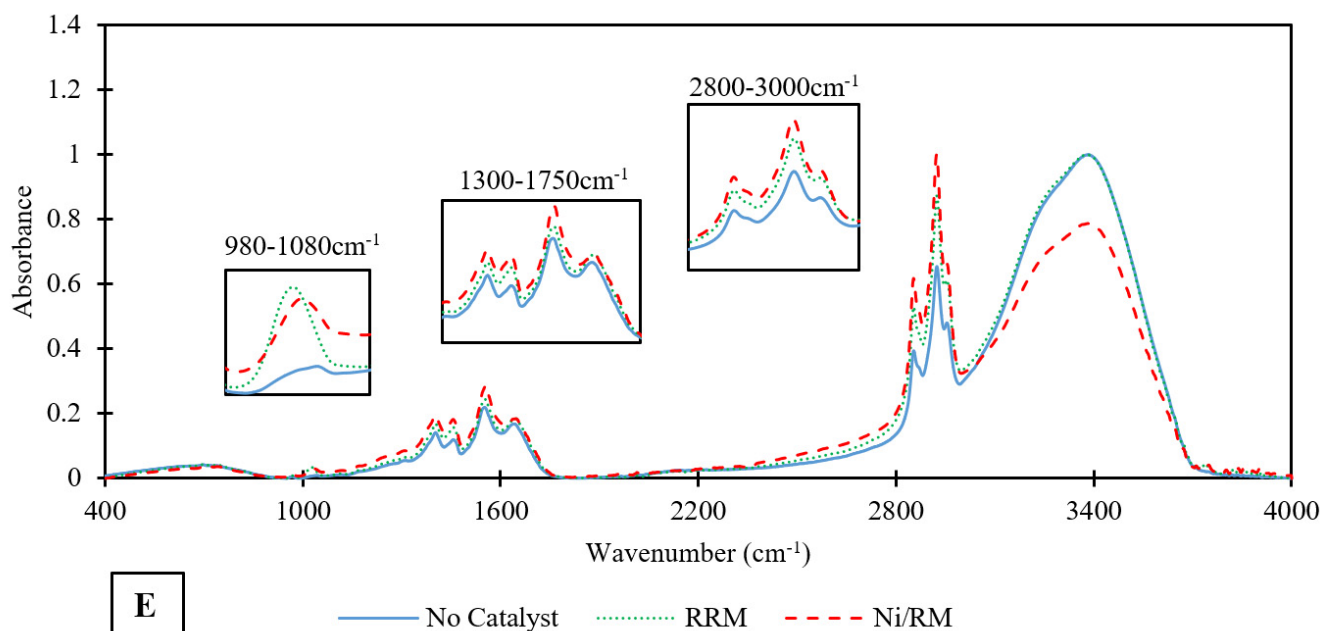


**Figure 4.** FTIR spectra of *Tetraselmis* biocrudes, (A)—non-catalytic reactions, (B)—reactions under nitrogen environment, (C)—reactions under ethylene environment, (D)—reactions under reducing environment and (E)—reactions under oxidizing environment.

#### NMR Analysis

Figure 5 illustrated the functional groups of *Tetraselmis* biocrudes generated under four reaction atmospheres from three different catalytic conditions, by semi-quantitative integration of  $^{13}\text{C}$  NMR spectra. The aliphatic groups found (such as methyl and methylene carbon atoms) within 0–28 ppm was assigned to saturated aliphatic groups where 28–55 ppm region was attributed to unsaturated aliphatic groups (separated from oxygen atoms by at least two bonds). The region of 55–95 ppm was designated to alcohols, esters, and anhydrous carbohydrates [56]. The reaction atmosphere significantly affected saturated aliphatic groups of biocrudes. The ethylene environment with Ni/RM catalyst has produced the highest saturated aliphatic groups percentage. The incorporation of catalyst has generated more saturated aliphatic compounds compared to non-catalytic reaction under reducing environment. According to absolute integral value (Supplementary Material, Table S5), Ni/RM catalyst produced 25.7% and 33% more saturated aliphatic groups in biocrudes than non-catalytic and RRM catalyst, respectively under reducing ambience. This finding agreed with the previous hydrodeoxygenation study by Ni/RM catalyst where incorporation of Ni metal increased the saturated aliphatic compounds in upgraded pinyon-juniper catalytic pyrolysis oil [50]. However, the absolute integral values of unsaturated and saturated aliphatic groups were almost same by Ni/RM catalyst in reducing atmosphere (Table S5). The RRM catalyst suppressed the unsaturated aliphatic groups of the biocrude by almost 2.5 times in reducing ambience. Therefore, it was evident that the RRM catalyst performed hydrogenation of unsaturated carbon in biocrude during HTL process under reducing environment [56]. The maximum alcohols, esters, and anhydrous carbohydrates were observed in the biocrudes from reducing-RRM condition. This result agreed with aliphatic ester region of FTIR biocrude spectra from the same reaction condition. The alcohols, esters, and anhydrous carbohydrates groups content were lower in all catalytic conditions under oxidizing environment compared to other three reaction environments. This finding agreed with the aliphatic ester region ( $980\text{--}1080\text{ cm}^{-1}$ ) of oxidizing environment (Figure 4A) where the oxidizing environment showed the minimum aliphatic esters peak in non-catalytic biocrude spectra.

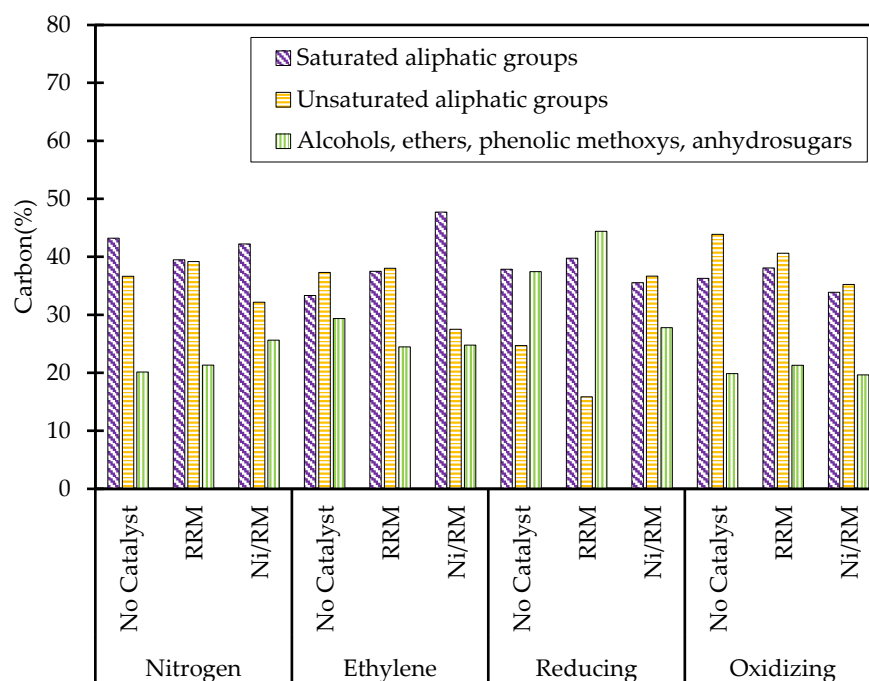


**Figure 5.** Functional group distribution in  $^{13}\text{C}$  NMR analysis of *Tetraselmis* biocrudes.

#### GC-MS Analysis

Table 3 has represented the GC-MS analysis of *Tetraselmis* derived HTL biocrude. The identified compounds with higher than 90% quality were selected for GC-MS analysis which covered 60% of total area percentages. A significant presence of long chain fatty acid (13–43% of area), alkenes (5.8–28% of area) along with nitrogenated compounds (2.9–8.1% of area), phenols (2.2–12.5% of area) and other oxygenates (2–11.8% of area) were detected in the *Tetraselmis* derived biocrude products. The abundance of long chain fatty acid and nitrogenated compounds were also observed in previous *Tetraselmis* HTL studies [57]. Algae generally contains fatty acid with high carbon number (14–22) which shows increased thermal stability during HTL conversion and remains intact in algal biocrude [58]. Among four non-catalytic conditions, a notable amount of fatty acid (n-hexadecanoic and oleic acid) was found in the biocrude produced under ethylene and oxidizing atmospheres. The fatty acid generally originates from the lipid fraction of algal feedstock which directly contributes to the HTL biocrude yield. During HTL conversion, the triglycerides from algal lipid hydrolyzed to free fatty acids due to the low dielectric constant of hot water [59]. The trend of biocrude yield in non-catalytic reactions in “3.3.1 Products yield distribution” section of this article was as follows: nitrogen > oxidizing > ethylene > reducing. It was reported that oxygen gas could facilitate the decomposition of softwood derived sugars during HTL conversion and enhanced organic acid production [60]. Most probably the ethylene and oxygen gases promoted fatty acid production under HTL condition and raised the biocrude yield in non-catalytic conversion. However, the algal biocrude from non-catalytic reaction under nitrogen environment contained notable amount of phenol with less fatty acid compared to other three gaseous atmospheres. It is difficult to conclude from this study, how different gases influenced the biocrude yield and composition. Besides lipid conversion, the interaction between algal building blocks (carbohydrates, lipid, protein) of *Tetraselmis* could be also responsible for biocrude yield enhancement under specific gaseous environment. More HTL experiments with model compounds of *Tetraselmis* feedstock are needed to reveal the reaction mechanism under certain gaseous environments.

**Table 3.** GC-MS analysis of *Tetraselmis* HTL biocrude.

Compounds	Chemical Formula	Area (%)											
		Nitrogen			Ethylene			Reducing			Oxidizing		
		No Catalyst	RRM	Ni/RM									
n-Hexadecanoic acid	C <sub>16</sub> H <sub>32</sub> O <sub>2</sub>	9.9	10.3	7.9	14.2	21.4	15.6	14.7	26.1	25.3	20.7	22.6	12.5
Oleic Acid	C <sub>18</sub> H <sub>34</sub> O <sub>2</sub>	6.0	10.9	6.0	10.3	12.9	20.7	8.7	17.6	10.9	10.0	16.6	14.6
Phenol, 2,2'-methylenebis[6-(1,1-dimethylethyl)-4-ethyl]-	C <sub>25</sub> H <sub>36</sub> O <sub>2</sub>	10.2	3.2	8.1	1.5	1.4	2.4	6.2	0.6	1.0	2.5	1.1	1.0
Phenol	C <sub>6</sub> H <sub>6</sub> O	2.3	0.7	2.6	2.0	1.3	0.6	<LOD	1.6	1.9	<LOD	1.4	1.2
2-Pentadecanone, 6,10,14-trimethyl-	C <sub>18</sub> H <sub>36</sub> O	4.3	2.0	2.5	3.6	2.1	0.8	3.3	1.6	1.9	4.8	1.4	1.6
Phenylethyl Alcohol	C <sub>8</sub> H <sub>10</sub> O	<LOD	<LOD	0.5	1.2	2.8	1.1	<LOD	2.3	1.6	<LOD	1.9	0.9
Isophytol	C <sub>20</sub> H <sub>40</sub> O	3.2	<LOD	<LOD	5.5	<LOD	0.5	6.7	<LOD	<LOD	3.6	<LOD	1.0
Dianhydromannitol	C <sub>6</sub> H <sub>10</sub> O <sub>4</sub>	<LOD	<LOD	1.0	1.5	<LOD	<LOD	1.1	<LOD	<LOD	<LOD	2.3	0.9
9H-Pyrido[3,4-b]indole, 1-methyl-	C <sub>12</sub> H <sub>10</sub> N	3.1	1.5	2.5	2.5	1.1	2.9	4.7	2.2	1.2	2.5	2.1	2.0
Pyridine, 3-phenyl-	C <sub>11</sub> H <sub>9</sub> N	<LOD	0.9	0.6	<LOD	0.2	0.2	<LOD	0.4	0.5	1.6	0.8	1.2
Indole	C <sub>8</sub> H <sub>7</sub> N	<LOD	0.8	1.9	1.2	0.6	0.5	<LOD	0.7	1.7	1.9	1.1	2.0
1H-Indole, 3-methyl-	C <sub>9</sub> H <sub>9</sub> N	<LOD	<LOD	1.0	0.8	0.4	<LOD	<LOD	0.7	1.0	<LOD	1.2	1.9
Quinoline, 1,2,3,4-tetrahydro-	C <sub>9</sub> H <sub>11</sub> N	<LOD	<LOD	0.6	1.0	0.6	0.5	<LOD	0.4	0.7	<LOD	0.4	1.0
2-Hexadecene, 3,7,11,15-tetramethyl-, [R-[R*,R*-(E)]]-	C <sub>20</sub> H <sub>40</sub>	21.0	28.6	24.7	13.9	15.6	13.6	14.7	5.8	10.2	14.0	6.1	16.4

\* &lt; LOD = &lt; Limit of Detection.

The alkene (2-hexadecene, 3,7,11,15-tetramethyl-, [R-[R\*,R\*-(E)]]-) detected in *Tetraselmis* biocrudes, might come from the decomposition of unsaturated fatty acids of algal feedstock [61]. The phenols and nitrogenated compounds including pyridine, indole, quinoline might originate from protein fraction of *Tetraselmis* by the decarboxylation and deamination reactions [62,63]. Besides phenols and organic acids, the other oxygenated compounds such as alcohol (isophytol, phenylethyl alcohol), ketones (2-Pentadecanone, 6,10,14-trimethyl-) and dianhydromannitol might source back to the polysaccharides and cellulose content of algae [61]. The catalyst played a role in elevating the total area percentage of the nitrogenated compounds in inert, reducing, and oxidizing reaction environments. Irrespective of reaction environments, the lower amount of oxygenates was also found in the biocrudes from catalytic conversion. The increasing nitrogen with suppressed oxygen content by catalytic HTL was also supported by the elemental composition of the biocrudes (Table 2). The minimum total area percentage of fatty acid (n-hexadecanoic acid and oleic acid) by Ni/RM catalyst under nitrogen environment, might be responsible for the lowest TAN value (Table 2) of the same biocrude. The RRM catalysts under reducing environment, suppressed the area percentage of alkene (2-Hexadecene, 3,7,11,15-tetramethyl-, [R-[R\*,R\*-(E)]]-) compared to Ni/RM and non-catalytic reaction. This finding agreed with the NMR result of lower unsaturated compounds by RRM catalyst under reducing atmosphere.

### 3.3.3. Analysis of Byproducts

Table 4 presents the analysis of three HTL byproducts: aqueous phase, solid residue, and gaseous phase. The aqueous phase was characterized by TOC, TN with NH<sub>4</sub><sup>+</sup>-N,

$\text{NO}_3^-$ -N, COD, and pH. Among the non-catalytic reactions, the reducing environment has maximized TOC of aqueous phase where the minimum was found in inert environment. This result suggested that the reducing ambience in the absence of catalyst solubilized some organic compounds into the aqueous phase. The addition of catalysts increased TOC value in the aqueous products. The highest TOC (16.41 g/L) was observed in the aqueous phase produced from oxidizing-Ni/RM reaction. Since pH of aqueous phase was not in acidic side for oxidizing-Ni/RM condition, the TOC increase was probably due to the formation of more hydroxyl groups from alcohols and low molecular weight phenolics. Almost 70% of TN was occupied by Org-N. The majority of Org-N in TN could be the confirmation of protein decomposition as the nitrogen source in aqueous phase [64]. Incorporation of catalysts increased the  $\text{NH}_4^+$ -N content of the aqueous products, and the highest amount was detected in oxidizing-RRM reaction. Both RRM and Ni/RM catalysts increased COD of the aqueous phases irrespective of reaction environments which indicated the negative effects of catalysts over aqueous phase treatment for reuse. The highest COD was observed in the aqueous product of reducing-Ni/RM reactions. The Ni/RM catalyst under reducing environment also reduced the pH value of the aqueous byproduct by 2–7% compared to other reactions of this study.

**Table 4.** Properties of *Tetraselmis* HTL byproducts.

	Nitrogen			Ethylene			Reducing			Oxidizing				
	No Cat- alyst	RRM	Ni/RM	No Cat- alyst	RRM	Ni/RM	No Cat- alyst	RRM	Ni/RM	No Cat- alyst	RRM	Ni/RM		
Aqueous Phase (g/L)	TOC	11.42 ± 1.00	13.19 ± 0.53	13.65 ± 0.20	12.53 ± 0.82	13.98 ± 1.50	13.79 ± 0.14	12.65 ± 1.31	13.26 ± 0.45	15.80 ± 0.38	12.06 ± 0.77	13.95 ± 0.89	16.41 ± 0.93	
	$\text{NH}_4^+$ -N	2.87 ± 0.34	4.00 ± 0.43	3.92 ± 0.22	2.71 ± 0.19	3.74 ± 0.36	2.83 ± 0.54	3.13 ± 0.46	3.15 ± 0.27	4.02 ± 0.43	3.00 ± 0.76	4.20 ± 0.45	3.64 ± 0.44	
	$\text{NO}_3^-$ -N	0.02 ± 0.00	0.06 ± 0.01	0.02 ± 0.00	0.01 ± 0.00	0.02 ± 0.00	0.05 ± 0.01	0.03 ± 0.00	0.02 ± 0.00	0.06 ± 0.02	0.02 ± 0.00	0.05 ± 0.01	0.06 ± 0.01	
	Org-N <sup>a</sup>	7.41 ± 0.16	7.24 ± 0.04	7.12 ± 0.54	7.54 ± 0.35	7.62 ± 0.40	7.83 ± 0.30	7.52 ± 0.17	7.37 ± 0.05	6.68 ± 0.40	6.98 ± 0.01	7.19 ± 0.28	7.86 ± 0.01	
	TN	10.30 ± 0.50	11.30 ± 0.48	11.06 ± 0.76	10.26 ± 0.54	11.38 ± 0.76	10.71 ± 0.85	10.68 ± 0.63	10.54 ± 0.32	10.76 ± 0.85	10.00 ± 0.75	11.44 ± 0.18	11.56 ± 0.46	
	COD	86.00 ± 0.30	99.60 ± 0.01	89.20 ± 0.10	87.60 ± 0.10	110.0 ± 0.11	96.40 ± 3.61	89.90 ± 0.23	101.10 ± 0.82	119.10 ± 0.22	91.20 ± 0.31	103.00 ± 0.21	107.60 ± 0.12	
	pH	8.30 ± 0.60	8.60 ± 0.10	8.40 ± 0.31	8.70 ± 0.12	8.30 ± 0.52	8.70 ± 0.22	8.30 ± 0.20	8.50 ± 0.10	7.90 ± 0.10	8.20 ± 0.20	8.10 ± 0.10	8.20 ± 0.30	
Solid Residue (wt%)	C	34.2 ± 2.3	25.1 ± 0.1	21.1 ± 1.4	36.9 ± 0.1	18.3 ± 1.0	22.5 ± 0.1	28.9 ± 0.9	20.7 ± 0.3	18.0 ± 0.2	37.4 ± 1.6	24.9 ± 1.4	24.7 ± 0.1	
	H	4.8 ± 0.1	2.7 ± 0.1	2.5 ± 0.2	4.4 ± 0.1	2.1 ± 0.2	2.4 ± 0.1	3.4 ± 0.2	1.9 ± 1.4	2.7 ± 0.1	3.5 ± 0.6	3.4 ± 0.3	3.2 ± 0.1	
	N	2.3 ± 0.2	1.6 ± 0.1	1.4 ± 0.1	2.2 ± 0.1	1.3 ± 0.1	1.5 ± 0.4	1.9 ± 0.1	1.4 ± 0.1	1.2 ± 0.1	2.8 ± 0.1	1.8 ± 0.2	1.8 ± 0.1	
	S	0.3 ± 0.1	0.5 ± 0.1	1.2 ± 0.1	0.4 ± 0.2	0.4 ± 0.1	1.2 ± 0.1	0.3 ± 0.1	0.4 ± 0.1	1.4 ± 0.1	0.3 ± 0.1	0.4 ± 0.1	0.8 ± 0.2	
	Ash	55.4 ± 0.1	58.1 ± 0.2	64.3 ± 0.1	55.3 ± 0.3	68.5 ± 0.2	62.9 ± 0.4	59.6 ± 0.2	57.2 ± 0.1	70.5 ± 0.1	46.7 ± 0.1	47.8 ± 0.2	56.9 ± 0.3	
	O <sup>a</sup>	3.1 ± 2.8	12.0 ± 0.4	9.5 ± 1.8	0.9 ± 0.7	9.4 ± 1.5	9.6 ± 0.9	5.9 ± 1.3	18.4 ± 1.8	6.1 ± 0.4	9.4 ± 2.4	21.8 ± 2.1	12.6 ± 0.8	
Gas Composition (mol%)	H <sub>2</sub>	1.5 ± 0.0	6.1 ± 0.2	4.8 ± 0.1	1.1 ± 0.0	8.0 ± 0.1	6.7 ± 0.1		Consumed			1.0 ± 0.1	3.9 ± 0.2	2.5 ± 0.1
	CH <sub>4</sub>	0.1 ± 0.0	1.5 ± 0.1	0.1 ± 0.0	0.1 ± 0.0	1.4 ± 0.1	3.0 ± 0.1	0.1 ± 0.0	1.1 ± 0.1	0.1 ± 0.0	0.1 ± 0.0	0.7 ± 0.1	0.1 ± 0.0	
	CO	3.2 ± 0.1	0.8 ± 0.1	4.8 ± 0.1	2.2 ± 0.0	2.5 ± 0.1	0.1 ± 0.0	3.1 ± 0.1	2.4 ± 0.1	8.4 ± 0.1	1.7 ± 0.0	3.8 ± 0.2	2.9 ± 0.0	
	CO <sub>2</sub>	80.8 ± 0.9	62.1 ± 0.1	65.8 ± 0.3	72.7 ± 1.2	41.0 ± 1.6	58.7 ± 0.1	82.8 ± 0.8	67.5 ± 0.6	69.8 ± 0.2	85.1 ± 1.5	52.9 ± 0.5	72.7 ± 0.1	
	Balance <sup>a</sup>	14.4 ± 0.9	29.4 ± 0.3	24.6 ± 0.3	23.9 ± 1.3	47.1 ± 1.5	31.5 ± 0.1	14.0 ± 0.7	29.1 ± 0.8	21.8 ± 0.1	12.2 ± 1.5	38.1 ± 1.0	21.7 ± 0.1	
Gas Consumption (mol/kg feedstock)	0	0	0	0.11 ± 0.02	0.72 ± 0.2	1.48 ± 0.4	0.01 ± 0.0	0.04 ± 0.01	1.52 ± 0.3	1.22 ± 0.1	1.07 ± 0.2	1.23 ± 0.4		

<sup>a</sup> by difference.

The solid residues of this study were analyzed by elemental composition and the analysis results were presented as catalyst free basis (Equation (S1), Supplementary Material). The addition of catalyst clearly decreased the carbon content of solid chars compared to non-catalytic reaction. The carbon percentage of the char showed the opposite trend of biocrudes: Ni/RM < RRM < No Catalyst. It suggested that catalysts transferred the carbon from feedstock to biocrude rather than solid char. The lowered nitrogen content in catalyst derived solid char was the result of enhanced nitrogen content of biocrude and aqueous phase. Regardless of reaction environment, increased oxygen and sulfur was found in the solid residues of catalytic reactions which indicated that the RM based catalysts assisted the migration of oxygen and sulfur-based compounds from *Tetraselmis* feedstock to char by HTL treatment in inert, ethylene, reducing and oxidizing reaction environments. The catalysts also increased ash in the char under four reaction atmospheres. A similar phenomenon was observed in sewage sludge HTL study with reduced red mud catalysts under nitrogen and ethylene atmospheres [32].

The gas phase analysis only quantified H<sub>2</sub>, CH<sub>4</sub>, CO and CO<sub>2</sub> gases on a mol% basis (excluding reaction environment). The RRM catalyst has promoted in situ hydrogen production in nitrogen, ethylene and oxidizing ambiances. The hydrogen production maximized under ethylene environment by 1.3–7 mol%. The reaction ambience consumption was significantly high with Ni/RM catalyst in ethylene and hydrogen reaction atmospheres. Addition of catalysts suppressed the CO<sub>2</sub> production for all four reaction atmospheres. The maximum CO<sub>2</sub> production was observed from non-catalytic oxidizing environment which suggested that the decarboxylation is a dominant pathway in this condition.

### 3.4. Carbon and Nitrogen Distribution

Carbon distribution in the *Tetraselmis* HTL products is illustrated in Figure 6A. The carbon recovery was calculated based on the elemental analysis of *Tetraselmis* feedstock, biocrude, solid residue; TOC content of the aqueous phase and the mol fraction of CO, CO<sub>2</sub> and CH<sub>4</sub> gases (Equations (S2)–(S4), Supplementary Material). The carbon addition to the HTL system by ethylene atmosphere was calculated using the ethylene consumption rate from Table 4 (Equation (S3), Supplementary Material). The carbon mostly transferred from feedstock to biocrude products and carbon transfer was increased by catalytic reactions. The elemental analysis (Table 2) of the biocrudes and carbon distribution showed the identical carbon transfer trend: No Catalyst < RRM < Ni/RM. The carbon recovery in biocrudes was comparatively lower in oxidizing atmosphere. Therefore, the carbon transfer to solid residue and aqueous phase was increased by oxidizing environment. Irrespective of reaction environments, significant amount of carbon transferred to the “Balance” fractions of the non-catalytic reactions. Most probably more gases with higher carbon content were produced from those HTL reactions, which were not analyzed in this study. Moreover, increased CO<sub>2</sub> production (Table 4) from non-catalytic reactions under inert, ethylene and reducing reaction environments, was supported by the enhanced carbon transfer in gaseous phase.

Nitrogen distribution of *Tetraselmis* HTL products was presented in Figure 6B. The nitrogen distribution was calculated based on nitrogen content of feedstock, biocrude, solid residue from elemental analysis and TN value of aqueous phase. Almost 64–73% of the nitrogen ended up in the aqueous phase whereas 9–25% transferred to the biocrude. In this study, a notable amount of nitrogen transferred from algal feedstock to biocrudes and aqueous products. It was evident that the addition of catalysts promoted higher decomposition of the protein rich *Tetraselmis* feedstock during HTL process and the produced nitrogenated compounds distributed among the HTL products. The higher nitrogen content of biocrudes indicated that further upgrading process was required to use it as transportation fuel [65].

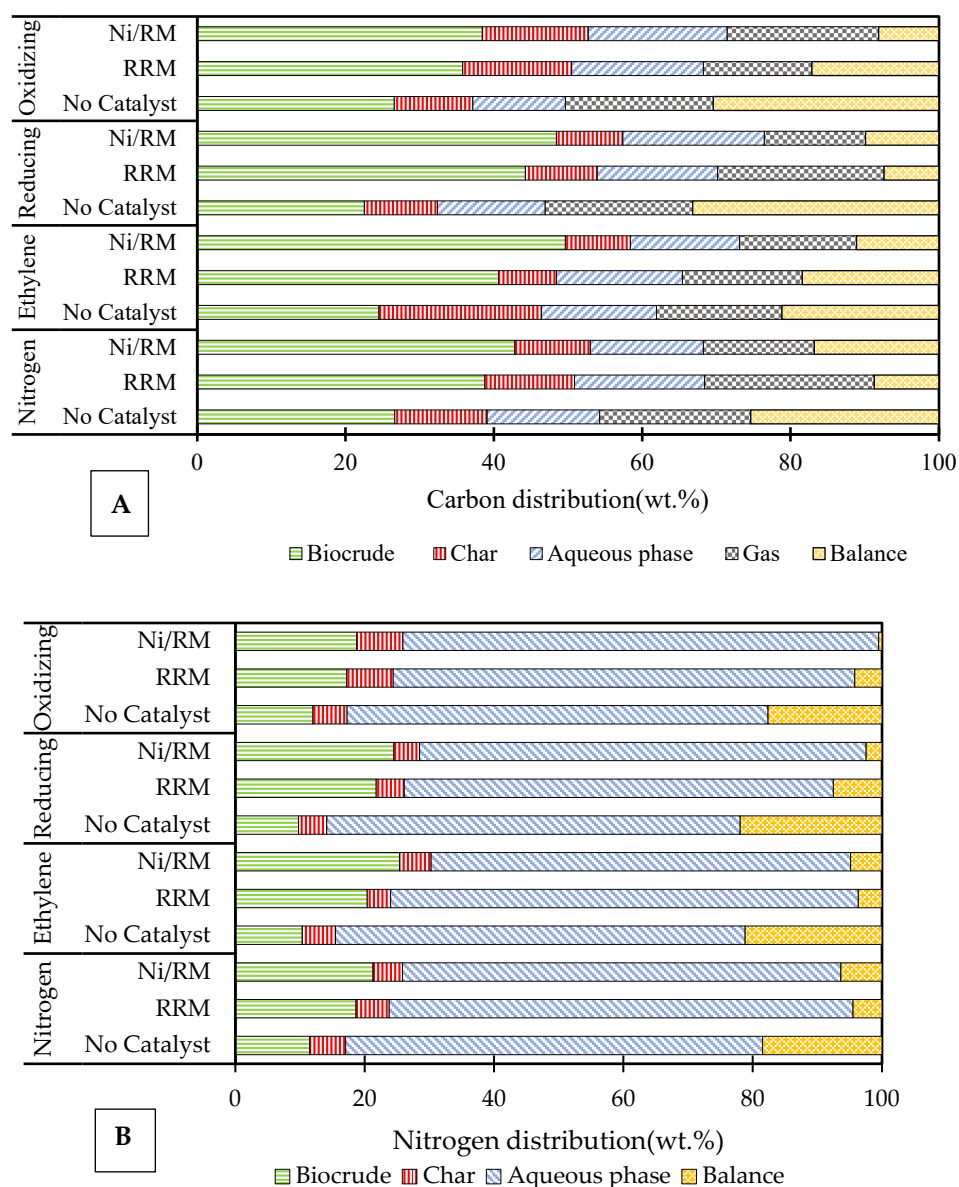


**Figure 6.** Carbon and nitrogen distribution in *Tetraselmis* HTL products, (A)—Carbon distribution, and (B)—Nitrogen distribution.

#### 4. Conclusions

The red mud (RM) based catalysts, reduced red mud (RRM) and red mud supported nickel (Ni/RM), were applied to hydrothermal liquefaction (HTL) of *Tetraselmis* sp. algae under nitrogen, ethylene, reducing and oxidizing reaction environments. Regardless of reaction environments, the use of catalysts has increased the yield of *Tetraselmis* derived biocrude. The highest biocrude yield of 37 wt.% was produced under ethylene environment with Ni/RM catalyst. Both RRM and Ni/RM catalysts promoted deoxygenation, reaction with increased carbon content and calorific value for the biocrude products in four reaction atmospheres. The Ni/RM catalyst under inert environment reduced biocrude acidity by 20–50% compared to other reaction conditions. The desulfurization activity of Ni/RM catalysts and demetallization effect of RRM catalyst were observed in all biocrude products, irrespective of reaction environments. A major portion of nitrogen migrated to aqueous phase from protein enriched *Tetraselmis* feedstock after HTL treatment where most of the carbon ended up in the biocrudes. Among the non-catalytic HTL reactions, inert environment maximized biocrude production from *Tetraselmis* feedstock, ethylene

environment lowered total acid number (TAN) of the biocrudes and reducing environment added maximum carbon and minimum oxygen and sulfur content to *Tetraselmis* biocrude.

**Supplementary Materials:** The following supporting information can be downloaded at: <https://www.mdpi.com/article/10.3390/en16010491/s1>. Table S1: ICP-OES analysis of feedstock (*Tetraselmis* sp.) and catalysts (RRM, Ni/RM); Table S2: Physisorption data of the catalysts; Table S3: F and p values from two-way ANOVA of *Tetraselmis* biocrude yields, carbon, sulfur, ash and oxygen content with reaction environment and catalysts as independent variables; Table S4: p values from Tukey HSD test for interaction between reaction environment and catalyst in carbon, ash, and oxygen content of *Tetraselmis* biocrude; Figure S1: <sup>13</sup>C NMR spectra of Ni/RM catalyst derived *Tetraselmis* biocrudes: A-Nitrogen, B-Ethylene, C-Reducing and D-Oxidizing reaction environments; Table S5: Functional group distribution in biocrudes from <sup>13</sup>C NMR spectral integration, Equation (S1): Calculation for catalyst free basis elemental composition of solid char, Equations (S2)–(S4): Calculation of carbon distribution among HTL products from *Tetraselmis* conversion.

**Author Contributions:** Conceptualization, S.A.; supervision, S.A.; funding acquisition, S.A.; methodology, T.R.; validation, S.A. and B.T.H.; formal analysis, F.F.-K.-N., T.-S.O. and Q.W.; investigation, T.R.; data curation, T.R., P.R. and B.T.H.; writing—original draft preparation, T.R.; writing—review and editing, T.R., H.J. and S.A.; visualization, T.R. and P.R. All authors have read and agreed to the published version of the manuscript.

**Funding:** Alabama Department of Economic and Community Affairs (ADECA-1ARDEF22 02), National Science Foundation (Award No.: 2119809), and Alabama Agricultural Experiment Station and the Hatch program (ALA014-1-19068) of the National Institute of Food and Agriculture, U.S. Department of Agriculture (USDA).

**Data Availability Statement:** The data presented in this study are available on request from the corresponding author.

**Conflicts of Interest:** The authors declare no conflict of interest. The funders had no role in the design of the study; in the collection, analyses, or interpretation of data; in the writing of the manuscript; or in the decision to publish the results.

## References

1. Peterson, A.A.; Vogel, F.; Lachance, R.P.; Fröling, M.; Michael, J.; Antal, J.; Tester, J.W. Thermochemical Biofuel Production in Hydrothermal Media: A Review of Sub- and Supercritical Water Technologies. *Energy Environ. Sci.* **2008**, *1*, 32–65. [CrossRef]
2. Elgarahy, A.M.; Hammad, A.; El-Sherif, D.M.; Abouzid, M.; Gaballah, M.S.; Elwakeel, K.Z. Thermochemical Conversion Strategies of Biomass to Biofuels, Techno-Economic and Bibliometric Analysis: A Conceptual Review. *J. Environ. Chem. Eng.* **2021**, *9*, 106503. [CrossRef]
3. Baloch, H.A.; Nizamuddin, S.; Siddiqui, M.T.H.; Riaz, S.; Jatoi, A.S.; Dumbre, D.K.; Mubarak, N.M.; Srinivasan, M.P.; Griffin, G.J. Recent Advances in Production and Upgrading of Bio-Oil from Biomass: A Critical Overview. *J. Environ. Chem. Eng.* **2018**, *6*, 5101–5118. [CrossRef]
4. Bi, Z.; Zhang, J.; Peterson, E.; Zhu, Z.; Xia, C.; Liang, Y.; Wiltowski, T. Biocrude from Pretreated Sorghum Bagasse through Catalytic Hydrothermal Liquefaction. *Fuel* **2017**, *188*, 112–120. [CrossRef]
5. Watson, J.; Wang, T.; Si, B.; Chen, W.-T.; Aierzhati, A.; Zhang, Y. Valorization of Hydrothermal Liquefaction Aqueous Phase: Pathways towards Commercial Viability. *Prog. Energy Combust. Sci.* **2020**, *77*, 100819. [CrossRef]
6. Shurin, J.B.; Abbott, R.L.; Deal, M.S.; Kwan, G.T.; Litchman, E.; McBride, R.C.; Mandal, S.; Smith, V.H. Industrial-Strength Ecology: Trade-Offs and Opportunities in Algal Biofuel Production. *Ecol. Lett.* **2013**, *16*, 1393–1404. [CrossRef]
7. Wang, S.; Zhao, S.; Uzoejinwa, B.B.; Zheng, A.; Wang, Q.; Huang, J.; Abomohra, A.E.-F. A State-of-the-Art Review on Dual Purpose Seaweeds Utilization for Wastewater Treatment and Crude Bio-Oil Production. *Energy Convers. Manag.* **2020**, *222*, 113253. [CrossRef]
8. Bhushan, S.; Kalra, A.; Simsek, H.; Kumar, G.; Prajapati, S.K. Current Trends and Prospects in Microalgae-Based Bioenergy Production. *J. Environ. Chem. Eng.* **2020**, *8*, 104025. [CrossRef]
9. Jazie, A.A.; Haydary, J.; Abed, S.A.; Al-Dawody, M.F. Hydrothermal Liquefaction of *Fucus Vesiculosus* Algae Catalyzed by H $\beta$  Zeolite Catalyst for Biocrude Oil Production. *Algal Res.* **2022**, *61*, 102596. [CrossRef]
10. Kandasamy, S.; Devarayan, K.; Bhuvanendran, N.; Zhang, B.; He, Z.; Narayanan, M.; Mathimani, T.; Ravichandran, S.; Pugazhendhi, A. Accelerating the Production of Bio-Oil from Hydrothermal Liquefaction of Microalgae via Recycled Biochar-Supported Catalysts. *J. Environ. Chem. Eng.* **2021**, *9*, 105321. [CrossRef]

11. Xia, J.; Han, L.; Zhang, C.; Guo, H.; Rong, N.; Baloch, H.A.; Wu, P.; Xu, G.; Ma, K. Hydrothermal Co-Liquefaction of Rice Straw and *Nannochloropsis*: The Interaction Effect on Mechanism, Product Distribution and Composition. *J. Anal. Appl. Pyrolysis* **2022**, *161*, 105368. [[CrossRef](#)]
12. Norouzi, O.; Mazhkoo, S.; Haddadi, S.A.; Arjmand, M.; Dutta, A. Hydrothermal Liquefaction of Green Macroalgae *Cladophora Glomerata*: Effect of Functional Groups on the Catalytic Performance of Graphene Oxide/Polyurethane Composite. *Catal. Today* **2022**, *404*, 93–104. [[CrossRef](#)]
13. Yu, J.; Audu, M.; Myint, M.T.; Cheng, F.; Jarvis, J.M.; Jena, U.; Nirmalakhandan, N.; Brewer, C.E.; Luo, H. Bio-Crude Oil Production and Valorization of Hydrochar as Anode Material from Hydrothermal Liquefaction of Algae Grown on Brackish Dairy Wastewater. *Fuel Process. Technol.* **2022**, *227*, 107119. [[CrossRef](#)]
14. Guo, B.; Yang, B.; Weil, P.; Zhang, S.; Hornung, U.; Dahmen, N. The Effect of Dichloromethane on Product Separation during Continuous Hydrothermal Liquefaction of *Chlorella Vulgaris* and Aqueous Product Recycling for Algae Cultivation. *Energy Fuels* **2022**, *36*, 922–931. [[CrossRef](#)]
15. Biswas, B.; Kumar, A.; Kaur, R.; Krishna, B.B.; Bhaskar, T. Co-Hydrothermal Liquefaction of Lignin and Macroalgae: Effect of Process Parameters on Product Distribution. *BioEnergy Res.* **2022**. [[CrossRef](#)]
16. Chen, J.; Zhang, J.; Pan, W.; An, G.; Deng, Y.; Li, Y.; Hu, Y.; Xiao, Y.; Liu, T.; Leng, S.; et al. A Novel Strategy to Simultaneously Enhance Bio-Oil Yield and Nutrient Recovery in Sequential Hydrothermal Liquefaction of High Protein Microalgae. *Energy Convers. Manag.* **2022**, *255*, 115330. [[CrossRef](#)]
17. Mishra, S.; Mohanty, K. Co-HTL of Domestic Sewage Sludge and Wastewater Treatment Derived Microalgal Biomass—An Integrated Biorefinery Approach for Sustainable Biocrude Production. *Energy Convers. Manag.* **2020**, *204*, 112312. [[CrossRef](#)]
18. Islam, M.B.; Khalekuzzaman, M.; Kabir, S.B.; Hossain, M.R.; Alam, M.A. Substituting Microalgal Biomass with Faecal Sludge for High-Quality Biocrude Production through Co-Liquefaction: A Sustainable Biorefinery Approach. *Fuel Process. Technol.* **2022**, *225*, 107063. [[CrossRef](#)]
19. Kim, Z.-H.; Park, H.; Lee, C.-G. Seasonal Assessment of Biomass and Fatty Acid Productivity by *Tetraselmis* sp. in the Ocean Using Semi-Permeable Membrane Photobioreactors. *J. Microbiol. Biotechnol.* **2016**, *26*, 1098–1102. [[CrossRef](#)]
20. Fon Sing, S.; Isdepsky, A.; Borowitzka, M.A.; Lewis, D.M. Pilot-Scale Continuous Recycling of Growth Medium for the Mass Culture of a Halotolerant *Tetraselmis* sp. in Raceway Ponds under Increasing Salinity: A Novel Protocol for Commercial Microalgal Biomass Production. *Bioresour. Technol.* **2014**, *161*, 47–54. [[CrossRef](#)]
21. Miyata, Y.; Sagata, K.; Hirose, M.; Yamazaki, Y.; Nishimura, A.; Okuda, N.; Arita, Y.; Hirano, Y.; Kita, Y. Fe-Assisted Hydrothermal Liquefaction of Lignocellulosic Biomass for Producing High-Grade Bio-Oil. *ACS Sustain. Chem. Eng.* **2017**, *5*, 3562–3569. [[CrossRef](#)]
22. Cao, J.-L.; Yan, Z.-L.; Deng, Q.-F.; Wang, Y.; Yuan, Z.-Y.; Sun, G.; Jia, T.-K.; Wang, X.-D.; Bala, H.; Zhang, Z.-Y. Mesoporous Modified-Red-Mud Supported Ni Catalysts for Ammonia Decomposition to Hydrogen. *Int. J. Hydrogen Energy* **2014**, *39*, 5747–5755. [[CrossRef](#)]
23. Saral, J.S.; Ranganathan, P. Catalytic Hydrothermal Liquefaction of *Spirulina Platensis* for Biocrude Production Using Red Mud. *Biomass Convers. Biorefinery* **2021**. [[CrossRef](#)]
24. Caprariis, B.D.; Damizia, M.; Tai, L.; Filippis, P.D. Hydrothermal Liquefaction of Biomass Using Waste Material as Catalyst: Effect on the Bio-Crude Yield and Quality. *Chem. Eng. Trans.* **2022**, *92*, 607–612. [[CrossRef](#)]
25. Zhang, W.; Liang, Y. Hydrothermal Liquefaction of Sewage Sludge—Effect of Four Reagents on Relevant Parameters Related to Biocrude and PFAS. *J. Environ. Chem. Eng.* **2022**, *10*, 107092. [[CrossRef](#)]
26. Pongsiriyakul, K.; Kiatkittipong, W.; Adhikari, S.; Lim, J.W.; Lam, S.S.; Kiatkittipong, K.; Dankeaw, A.; Reubroycharoen, P.; Laosiripojana, N.; Faungnawakij, K.; et al. Effective Cu/Re Promoted Ni-Supported  $\gamma$ -Al<sub>2</sub>O<sub>3</sub> Catalyst for Upgrading Algae Bio-Crude Oil Produced by Hydrothermal Liquefaction. *Fuel Process. Technol.* **2021**, *216*, 106670. [[CrossRef](#)]
27. Guo, B.; Walter, V.; Hornung, U.; Dahmen, N. Hydrothermal Liquefaction of *Chlorella Vulgaris* and *Nannochloropsis Gaditana* in a Continuous Stirred Tank Reactor and Hydrotreating of Biocrude by Nickel Catalysts. *Fuel Process. Technol.* **2019**, *191*, 168–180. [[CrossRef](#)]
28. Jahromi, H.; Agblevor, F.A. Hydrotreating of Guaiacol: A Comparative Study of Red Mud-Supported Nickel and Commercial Ni/SiO<sub>2</sub>-Al<sub>2</sub>O<sub>3</sub> Catalysts. *Appl. Catal. A Gen.* **2018**, *558*, 109–121. [[CrossRef](#)]
29. Peng, W.; Wu, C.; Wu, S.; Wu, Y.; Gao, J. The Effects of Reaction Atmosphere on Composition, Oxygen Distribution, and Heating Value of Products from the Hydrothermal Liquefaction of Corn Stalk. *Energy Sources Part A Recovery Util. Environ. Eff.* **2014**, *36*, 347–356. [[CrossRef](#)]
30. Wang, G.; Li, W.; Li, B.; Chen, H. Direct Liquefaction of Sawdust under Syngas. *Fuel* **2007**, *86*, 1587–1593. [[CrossRef](#)]
31. Yang, C.; Jia, L.; Chen, C.; Liu, G.; Fang, W. Bio-Oil from Hydro-Liquefaction of *Dunaliella Salina* over Ni/REHY Catalyst. *Bioresour. Technol.* **2011**, *102*, 4580–4584. [[CrossRef](#)] [[PubMed](#)]
32. Rahman, T.; Jahromi, H.; Roy, P.; Adhikari, S.; Hassani, E.; Oh, T.-S. Hydrothermal Liquefaction of Municipal Sewage Sludge: Effect of Red Mud Catalyst in Ethylene and Inert Ambiences. *Energy Convers. Manag.* **2021**, *245*, 114615. [[CrossRef](#)]
33. Channiwala, S.A.; Parikh, P.P. A Unified Correlation for Estimating HHV of Solid, Liquid and Gaseous Fuels. *Fuel* **2002**, *81*, 1051–1063. [[CrossRef](#)]

34. Roy, P.; Jahromi, H.; Adhikari, S.; Zou Finfrock, Y.; Rahman, T.; Ahmadi, Z.; Mahjouri-Samani, M.; Feyzbar-Khalkhali-Nejad, F.; Oh, T.-S. Performance of Biochar Assisted Catalysts during Hydroprocessing of Non-Edible Vegetable Oil: Effect of Transition Metal Source on Catalytic Activity. *Energy Convers. Manag.* **2022**, *252*, 115131. [[CrossRef](#)]
35. Harun, K.; Adhikari, S.; Jahromi, H. Hydrogen Production via Thermocatalytic Decomposition of Methane Using Carbon-Based Catalysts. *RSC Adv.* **2020**, *10*, 40882–40893. [[CrossRef](#)]
36. Jahromi, H.; Adhikari, S.; Roy, P.; Hassani, E.; Pope, C.; Oh, T.-S.; Karki, Y. Production of Green Transportation Fuels from Brassica Carinata Oil: A Comparative Study of Noble and Transition Metal Catalysts. *Fuel Process. Technol.* **2021**, *215*, 106737. [[CrossRef](#)]
37. RStudio Team. *RStudio: Integrated Development Environment for R*; RStudio Team: Boston, MA, USA, 2019.
38. Jahromi, H.; Adhikari, S.; Roy, P.; Shelley, M.; Hassani, E.; Oh, T.-S. Synthesis of Novel Biolubricants from Waste Cooking Oil and Cyclic Oxygenates through an Integrated Catalytic Process. *ACS Sustain. Chem. Eng.* **2021**, *9*, 13424–13437. [[CrossRef](#)]
39. Wang, Q.; Prasad, R.; Higgins, B.T. Aerobic Bacterial Pretreatment to Overcome Algal Growth Inhibition on High-Strength Anaerobic Digestates. *Water Res.* **2019**, *162*, 420–426. [[CrossRef](#)]
40. Wang, P.; Peng, H.; Adhikari, S.; Higgins, B.; Roy, P.; Dai, W.; Shi, X. Enhancement of Biogas Production from Wastewater Sludge via Anaerobic Digestion Assisted with Biochar Amendment. *Bioresour. Technol.* **2020**, *309*, 123368. [[CrossRef](#)]
41. Vo, T.K.; Kim, S.-S.; Ly, H.V.; Lee, E.Y.; Lee, C.-G.; Kim, J. A General Reaction Network and Kinetic Model of the Hydrothermal Liquefaction of Microalgae *Tetraselmis* sp. *Bioresour. Technol.* **2017**, *241*, 610–619. [[CrossRef](#)]
42. Eboibi, B.E.; Lewis, D.M.; Ashman, P.J.; Chinnasamy, S. Effect of Operating Conditions on Yield and Quality of Biocrude during Hydrothermal Liquefaction of Halophytic Microalga *Tetraselmis* sp. *Bioresour. Technol.* **2014**, *170*, 20–29. [[CrossRef](#)] [[PubMed](#)]
43. Shakya, R.; Whelen, J.; Adhikari, S.; Mahadevan, R.; Neupane, S. Effect of Temperature and Na<sub>2</sub>CO<sub>3</sub> Catalyst on Hydrothermal Liquefaction of Algae. *Algal Res.* **2015**, *12*, 80–90. [[CrossRef](#)]
44. Eboibi, B.E.-O.; Lewis, D.M.; Ashman, P.J.; Chinnasamy, S. Hydrothermal Liquefaction of Microalgae for Biocrude Production: Improving the Biocrude Properties with Vacuum Distillation. *Bioresour. Technol.* **2014**, *174*, 212–221. [[CrossRef](#)]
45. Jahromi, H.; Rahman, T.; Roy, P.; Adhikari, S. Hydrotreatment of Solvent-Extracted Biocrude from Hydrothermal Liquefaction of Municipal Sewage Sludge. *Energy Convers. Manag.* **2022**, *263*, 115719. [[CrossRef](#)]
46. Roy, P.; Jahromi, H.; Rahman, T.; Adhikari, S.; Feyzbar-Khalkhali-Nejad, F.; Barbary Hassan, E.; Oh, T.-S. Understanding the Effects of Feedstock Blending and Catalyst Support on Hydrotreatment of Algae HTL Biocrude with Non-Edible Vegetable Oil. *Energy Convers. Manag.* **2022**, *268*, 115998. [[CrossRef](#)]
47. Jones, S.B.; Zhu, Y.; Anderson, D.B.; Hallen, R.T.; Elliott, D.C.; Schmidt, A.J.; Albrecht, K.O.; Hart, T.R.; Butcher, M.G.; Drennan, C.; et al. *Process Design and Economics for the Conversion of Algal Biomass to Hydrocarbons: Whole Algae Hydrothermal Liquefaction and Upgrading*; U.S. Department of Energy Bioenergy Technologies Office: Washington, DC, USA, 2014; Report No. 23227.
48. Wang, W.; Xu, Y.; Wang, X.; Zhang, B.; Tian, W.; Zhang, J. Hydrothermal Liquefaction of Microalgae over Transition Metal Supported TiO<sub>2</sub> Catalyst. *Bioresour. Technol.* **2018**, *250*, 474–480. [[CrossRef](#)]
49. Li, H.; Hu, J.; Zhang, Z.; Wang, H.; Ping, F.; Zheng, C.; Zhang, H.; He, Q. Insight into the Effect of Hydrogenation on Efficiency of Hydrothermal Liquefaction and Physico-Chemical Properties of Biocrude Oil. *Bioresour. Technol.* **2014**, *163*, 143–151. [[CrossRef](#)]
50. Jahromi, H.; Agblevor, F.A. Hydrodeoxygenation of Pinyon-Juniper Catalytic Pyrolysis Oil Using Red Mud-Supported Nickel Catalysts. *Appl. Catal. B Environ.* **2018**, *236*, 1–12. [[CrossRef](#)]
51. Duan, P.; Savage, P.E. Hydrothermal Liquefaction of a Microalga with Heterogeneous Catalysts. *Ind. Eng. Chem. Res.* **2011**, *50*, 52–61. [[CrossRef](#)]
52. Sushil, S.; Batra, V.S. Catalytic Applications of Red Mud, an Aluminium Industry Waste: A Review. *Appl. Catal. B Environ.* **2008**, *81*, 64–77. [[CrossRef](#)]
53. Stigter, J.B.; de Haan, H.P.M.; Guicherit, R.; Dekkers, C.P.A.; Daane, M.L. Determination of Cadmium, Zinc, Copper, Chromium and Arsenic in Crude Oil Cargoes. *Environ. Pollut.* **2000**, *107*, 451–464. [[CrossRef](#)] [[PubMed](#)]
54. Gazulla, M.F.; Rodrigo, M.; Orduña, M.; Ventura, M.J.; Andreu, C. Determination of Phosphorus in Crude Oil and Middle Distillate Petroleum Products by Inductively Coupled Plasma–Optical Emission Spectrometry. *Anal. Lett.* **2017**, *50*, 2465–2474. [[CrossRef](#)]
55. Han, Y.; Hoekman, K.; Jena, U.; Das, P. Use of Co-Solvents in Hydrothermal Liquefaction (HTL) of Microalgae. *Energies* **2020**, *13*, 124. [[CrossRef](#)]
56. Zhang, X.; Chen, L.; Kong, W.; Wang, T.; Zhang, Q.; Long, J.; Xu, Y.; Ma, L. Upgrading of Bio-Oil to Boiler Fuel by Catalytic Hydrotreatment and Esterification in an Efficient Process. *Energy* **2015**, *84*, 83–90. [[CrossRef](#)]
57. Eboibi, B.E.; Lewis, D.M.; Ashman, P.J.; Chinnasamy, S. Influence of Process Conditions on Pretreatment of Microalgae for Protein Extraction and Production of Biocrude during Hydrothermal Liquefaction of Pretreated *Tetraselmis* sp. *RSC Adv.* **2015**, *5*, 20193–20207. [[CrossRef](#)]
58. Gu, X.; Martinez-Fernandez, J.S.; Pang, N.; Fu, X.; Chen, S. Recent Development of Hydrothermal Liquefaction for Algal Biorefinery. *Renew. Sustain. Energy Rev.* **2020**, *121*, 109707. [[CrossRef](#)]
59. Guo, Y.; Yeh, T.; Song, W.; Xu, D.; Wang, S. A Review of Bio-Oil Production from Hydrothermal Liquefaction of Algae. *Renew. Sustain. Energy Rev.* **2015**, *48*, 776–790. [[CrossRef](#)]
60. Sipponen, M.H.; Özdenkci, K.; Muddassar, H.R.; Melin, K.; Golam, S.; Oinas, P. Hydrothermal Liquefaction of Softwood: Selective Chemical Production Under Oxidative Conditions. *ACS Sustain. Chem. Eng.* **2016**, *4*, 3978–3984. [[CrossRef](#)]

61. Zhou, D.; Zhang, L.; Zhang, S.; Fu, H.; Chen, J. Hydrothermal Liquefaction of Macroalgae *Enteromorpha Prolifera* to Bio-Oil. *Energy Fuels* **2010**, *24*, 4054–4061. [[CrossRef](#)]
62. Biller, P.; Ross, A.B. Potential Yields and Properties of Oil from the Hydrothermal Liquefaction of Microalgae with Different Biochemical Content. *Bioresour. Technol.* **2011**, *102*, 215–225. [[CrossRef](#)]
63. Toor, S.S.; Rosendahl, L.; Rudolf, A. Hydrothermal Liquefaction of Biomass: A Review of Subcritical Water Technologies. *Energy* **2011**, *36*, 2328–2342. [[CrossRef](#)]
64. Han, Y.; Hoekman, S.K.; Cui, Z.; Jena, U.; Das, P. Hydrothermal Liquefaction of Marine Microalgae Biomass Using Co-Solvents. *Algal Res.* **2019**, *38*, 101421. [[CrossRef](#)]
65. Jazrawi, C.; Biller, P.; Ross, A.B.; Montoya, A.; Maschmeyer, T.; Haynes, B.S. Pilot Plant Testing of Continuous Hydrothermal Liquefaction of Microalgae. *Algal Res.* **2013**, *2*, 268–277. [[CrossRef](#)]

**Disclaimer/Publisher’s Note:** The statements, opinions and data contained in all publications are solely those of the individual author(s) and contributor(s) and not of MDPI and/or the editor(s). MDPI and/or the editor(s) disclaim responsibility for any injury to people or property resulting from any ideas, methods, instructions or products referred to in the content.